Adv. Manuf. (2020) 8:279–315
https://doi.org/10.1007/s40436-020-00313-2

A review on conventional and nonconventional machining of SiC particle-reinforced aluminium matrix composites

Ji-Peng Chen[1,2] · Lin Gu[3] · Guo-Jian He[3]

Received: 28 December 2019 / Revised: 28 March 2020 / Accepted: 5 June 2020 / Published online: 24 July 2020

Abstract Among the various types of metal matrix composites, SiC particle-reinforced aluminum matrix composites (SiC_p/Al) are finding increasing applications in many industrial fields such as aerospace, automotive, and electronics. However, SiC_p/Al composites are considered as difficult-to-cut materials due to the hard ceramic reinforcement, which causes severe machinability degradation by increasing cutting tool wear, cutting force, etc. To improve the machinability of SiC_p/Al composites, many techniques including conventional and nonconventional machining processes have been employed. The purpose of this study is to evaluate the machining performance of SiC_p/Al composites using conventional machining, i.e., turning, milling, drilling, and grinding, and using nonconventional machining, namely electrical discharge machining (EDM), powder mixed EDM, wire EDM, electrochemical machining, and newly developed high-efficiency machining technologies, e.g., blasting erosion arc machining. This research not only presents an overview of the machining aspects of SiC_p/Al composites using various processing technologies but also establishes optimization parameters as reference of industry applications.

✉ Ji-Peng Chen
cjp@njfu.edu.cn

[1] School of Mechanical and Electronic Engineering, Nanjing Forestry University, Nanjing 210037, People's Republic of China

[2] Department of Mechanical Engineering, Polytechnic University of Milan, Piazza Leonardo da Vinci 32, Milan 20133, Italy

[3] State Key Laboratory of Mechanical System and Vibration, School of Mechanical Engineering, Shanghai Jiao Tong University, Shanghai 200240, People's Republic of China

Keywords SiC_p/Al · Machining · Conventional · Wear mechanism · Nonconventional · Performance

1 Introduction

Metal matrix composites (MMCs) are prepared by combining a metallic matrix with hard ceramic reinforcements. Usually, metals including aluminum, magnesium, cobalt, titanium, copper, and various alloys of these materials can be adopted as a matrix. Meanwhile, the reinforcement material is generally a hard ceramic material, such as SiC, TiC, B_4C [1], Si_3N_4, AlN, Al_2O_3, TiB_2, ZrO_2, and Y_2O_3 [2]. The most widely used metal matrix materials for producing MMCs are aluminum and its alloys, because their ductility, formability, and low density can be combined with the stiffness and load-bearing capacity of the reinforcement [3]. Among numerous reinforcement materials, SiC is usually employed because it has some unique advantages, e.g., low cost, good hardness, and high corrosion resistance, compared to other reinforcements [4]. With the combined advantages of aluminum matrix materials and SiC reinforcement, SiC_p/Al MMCs have been certified and are steadily advancing owing to their excellent properties such as high strength, low density, and high wear resistance. They are widely used in the automobile and aircraft industries, structural applications, and many other systems [5]. Since SiC_p/Al composites consist of a metal matrix and a SiC reinforcement, different volume or weight percentage SiC in the matrix materials forms different SiC_p/Al composites, e.g., 10% (mass fraction), 20% (volume fraction), 45% (mass fraction) and 65% (volume fraction) SiC_p/Al matrix composites. A typical micrograph of a SiC_p/Al MMC with 65% (volume fraction) SiC particle reinforcement is shown in Fig. 1 [6].

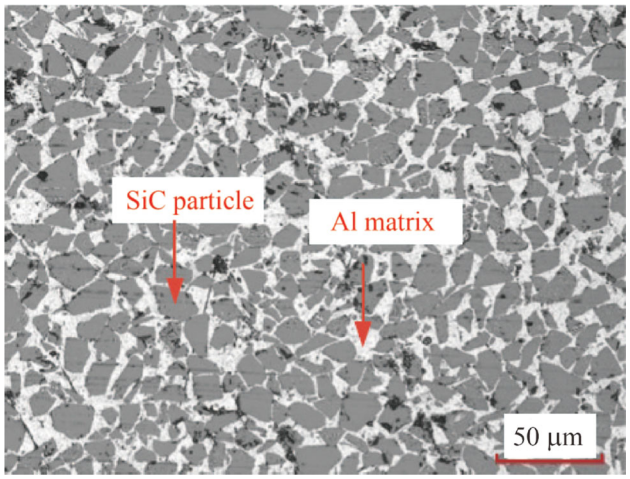

Fig. 1 Micrograph of 65% (volume fraction) SiC_p/Al matrix composite [6]

The specific properties of SiC make it very suitable for the production of Al MMCs [7]. However, on the processing aspect, the hard reinforcement causes an inevitable and severe problem of limiting the machining performance and rapid tool wear [8], which results in poor machin ability and cost increase [9]. Consequently, it is not surprising that SiC_p/Al composites are considered difficult-to-machine [10]. To date, many attempts have been made to improve the machinability of this hard material. Figure 2a indicates a steady increase in the number of studies on the machining of SiC_p/Al composites based on available publications since the 1990s. Figure 2b depicts the distribution of SiC_p/Al machinability studies conducted in industrial countries. In Fig. 3a, the statistics of the studied SiC (volume or weight fraction) according to appearance frequency in the literature are presented, and the SiC fractions are classified into 10 divisions. It is indicated that most studies are focused on SiC_p/Al composites with low SiC fractions, e.g., 5%–20% (volume fraction). Nevertheless, in recent years, increasing attention has been paid to the machining investigation of SiC_p/Al with high-SiC fractions, such as 50%, 56% and 65% (volume fraction).

Both conventional and nonconventional machining methods have been adopted for the processing of SiC_p/Al matrix composites. Figure 3b displays the approximate distribution of the machining methods utilized in the studies. It can be observed that turning, milling, and drilling are the most commonly used conventional machining technologies, whereas electrical discharge machining (EDM) is the most frequently used nonconventional machining technology. Besides EDM, wire EDM, and electrochemical machining (ECM), there are some other nonconventional machining technologies that have been adopted for improving the machining of SiC_p/Al matrix composites, e.g., the newly developed arc discharge

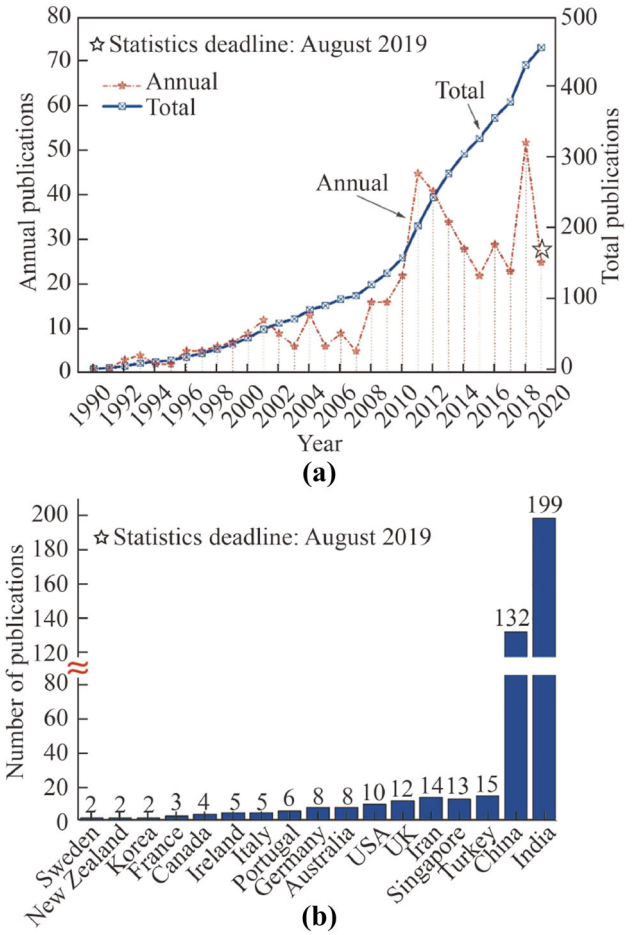

Fig. 2 **a** Publications of SiC_p/Al composite machining performance studies sourced from available databases and **b** distribution of industrial countries conducting SiC_p/Al composite machining investigations based on available literature

machining (ADM) [11]. This review considers both conventional and nonconventional machining studies conducted by numerous researchers to summarize the machinability performance of SiC_p/Al matrix composites and to offer transferable knowledge for industry application.

2 Fabrication and properties of SiC_p/Al matrix composites

2.1 Fabrication

Different fabrication techniques are used for the preparation of aluminum MMCs, e.g., stir casting, powder metallurgy, squeeze casting, in-situ process, deposition technique, and electroplating [12]. The widely used processes are stir casting and squeeze casting [13]. Stir casting (vortex technique) is generally considered as the most

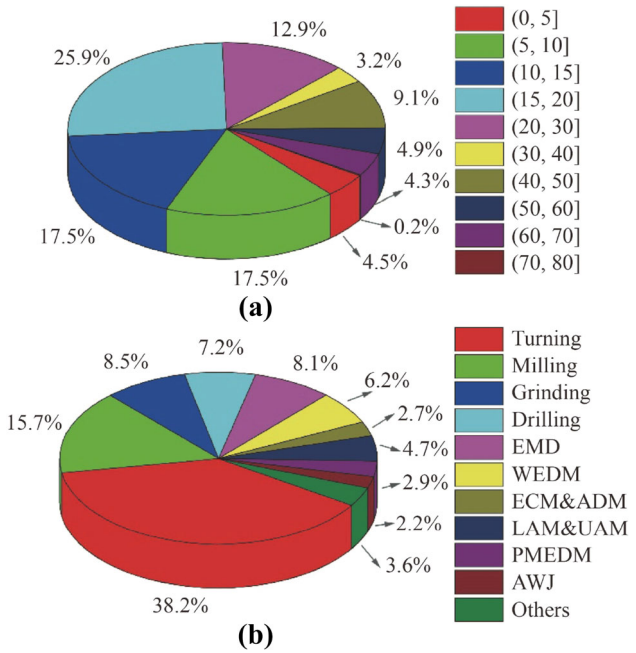

Fig. 3 **a** Percentage statistics of studied SiC fractions and **b** distribution of machining methods utilized in studies based on available database

economical one among all the available methods of Al MMC production, and it allows fabrication of very large components. Its advantages lie in simplicity, flexibility, and applicability to large volume production [14]. In this process, the matrix material is superheated above its melting temperature. The particles are also preheated at approximately 1 000–1 200 °C to oxidize the surface. The melted matrix is then stirred at an average stirring speed of 300–400 r/min as the vortex is formed during stirring [2, 15]. The major problem with stir casting is segregation or dusting of reinforced particles [13]. The squeeze casting process combines casting and forging to overcome casting defects such as pitting, porosity, and segregation of reinforcements [16]. Squeeze casting is a nonconventional process. Solidification of the molten slurry is carried out at high squeezing pressures, which enhance the microstructure and mechanical properties [17, 18]. In the fabrication of Al MMCs, many types of aluminum alloys have been adopted, e.g., Al6061 [19], AA2124 [20], Al7039 [21], Al7075 [22], Al A359 [23], Al A356 [24], Al6351 [25], and Al2124 [26], as matrix materials.

2.2 Properties

The machinability of MMCs differs from conventional metal materials because of the abrasive reinforcement element. It is known that SiC particles have some specific properties, e.g., high melting point (2 730 °C), high modulus (250 GPa), good thermal stability, good hardness, high wear and impact resistance, and high chemical resistance [7]. These excellent properties enhance the characteristics of Al-SiC composites. Consequently, SiC-related issues (e.g., fraction and size) are the key factors that are affecting the properties of SiC_p/Al matrix composites. It is believed that the mechanical properties of Al/SiC composites can be improved by increasing the volume fraction of SiC particles in the composites [27]. The yield strength and tensile strength increase with an increase in the SiC volume fraction; however, the plasticity [28] and impact toughness of the composites [29] deteriorate. Moreover, an increase in particle size reduces the strength but increases the composite ductility [30]; thus, a finer particle size of SiC offers a greater compressive strength [31]. Hong et al. [32] showed the variation in yield strength and ultimate tensile strength of composites as a function of the volume percentage of SiC: the yield strength ranged from 75 MPa (0% SiC-2014Al) to 210 MPa (10% (volume fraction) SiC-2014Al) and the ultimate tensile strength ranges from 185 MPa (0%SiC-2014Al) to 308 MPa(10% (volume fraction) SiC-2014Al). Yan et al. [33] produced Al matrix composites with high-volume fractions (55%–57%) of SiC particles using a new pressureless infiltration fabrication technology and described the properties of the SiC/Al composites as follows: density was 2.94 g/cm^3; elastic modulus was 220 GPa; flexure strength was 405 MPa; coefficient of thermal expansion (CTE) was 8.0×10^{-6}/K; thermal conductivity (TC) was 235.0 W/(m·K); Poisson's ratio was 0.23; and HV hardness was 200 N/mm^2. Huang et al. [34] fabricated 30% (volume fraction) SiC/6061Al composites using a pressureless sintering technique, and obtained the following properties: bending strength was 425.6 MPa; TC was 159 W/(m·K); and CTE was 1.25×10^{-5}/(20–100 °C). Tailor et al. [7] summarized the properties of SiC_p/Al composites as follows: bending strength was 350–500 MPa; elastic modulus was 200–300 GPa; and CTE was $(6.5–9.5) \times 10^{-6}$/K.

3 Conventional machining of SiC_p/Al matrix composites

3.1 Turning

3.1.1 Tool selection

The majority of SiC_p/Al turning investigations were conducted on lathes with a series of tools, such as uncoated tungsten carbide (WC) tools, polycrystalline diamond (PCD) tools [35], high-speed steel (HSS) cutting tools [36], cubic boron nitride (CBN) inserts tools [37, 38], single-crystal diamond (SCD) tools [39], TiN-coated hard carbide

tools, chemical vapor deposition (CVD) diamond tools, and multilayer-coated carbide insert tools [40].

PCD cutters are the most commonly used tools. They are generally preferentially considered when turning high-volume fraction SiC_p/Al composites. This is because these diamond-based turning tools both increase tool life and produce acceptable machining surfaces [41]. Durante et al. [42] insisted that it was possible to use only the PCD turning tools for improving the cutter service time and reducing the cutter changing frequency because HSS cutters could be destroyed in several seconds, whereas conventional and coated carbides could only work for a few minutes. Karabulut and Karako [43] also advised that PCD cutting tools should be used considering their excellent mechanical properties, although these tools were generally not cheap. On the aspect of tool cost, carbide and rhombic inserts have been regarded as an economical alternative turning solution compared to PCD or CBN tools. Sahin [44] reported that multicoated carbide tools with TiN as the top layer presented a better wear property than those of other cutting tools when machining SiC_p/Al matrix composites. In addition, Errico and Calzavarini [45] found that the deposition of a thin-film CVD diamond increased the cutting performance of hard metal substrates by more than 100%. Meanwhile, Andrewes et al. [46] observed a faster flank wear rate on a CVD diamond insert than on a PCD insert, but that faster wear rate could be reduced by securing stronger adhesion between the carbide substrate and diamond coating.

3.1.2 Tool wear mechanism

The machinability of MMCs differs from that of conventional materials due to the heavy cutting tool wear caused by abrasive elements [29]. Flank wear is the main type of wear observed on the tip tool [47]. In terms of tool wear mechanism, Manna and Bhattacharayya [48] explained the following: as the SiC particle contacted with the cutting tool, the atoms from the harder material were likely to diffuse into the softer matrix during the sliding process, which increased the hardness and abrasiveness of the workpiece. In the rapid wear phase and steady wear phase, diffusion and abrasion caused tool flank wear, respectively.

For the PCD tool, the tool wear that occurs on the cutter is similar to that observed when machining other materials and may be interpreted as surface fatigue and a microfracture process. The wear may be exacerbated by adhesion between the tool and the workpiece [49], and vertical grooves are visible on the flank face of the tool [50]. For the TiN-coated tool, abrasion is the main tool wear mechanism and there is almost no evidence of chemical wear; moreover, tool wear occurs on the flank face and the cutting speed is found to be the most influential parameter [51]. For the CVD diamond-coated carbide tool, the tool wear process includes melting of the workpiece material onto the tool surface as well as alterations of the rake face and cutting edge by the consequent pullout. Tool failure of smooth coatings occurs by a process including work material transfer and welding on the tool surface as well as regular removal of the built-up layer and built-up edge (BUE), inducing coating pullout, which exposes the relatively soft tool substrate to abrasive wear caused by the hard SiC particles [52]. For the uncoated WC tool, the flank wear is high due to the formation of BUE and generation of high cutting forces at low cutting speeds. In addition, the formation of BUE enlarges the actual rake angle; thus, it is found that the increment of cutting forces may increase the cutting tool wear in turn [53]. Manna and Bhattacharayya [54] proposed that the feed rate was less sensitive to tool wear compared with the cutting speed during turning SiC_p/Al with an uncoated WC cutter. For the CBN and diamond-coated cemented carbide cutting tools, abrasion and adhesion were observed as the predominant wear mechanisms. Scanning electron microscopy (SEM) investigation revealed that tool flank wear was the dominant wear mode. In contrast, machining of an MMC containing relatively large SiC particles (110 μm) using CBN cutting tools resulted in fracture of both the cutting edge and nose [55]. For the SCD tool, microwear, chipping, cleavage, abrasive wear, and chemical wear were the dominant wear patterns. It was pointed out that the combined effects of abrasive wear of SiC particles and catalysis of copper in the aluminum matrix had caused severe graphitization. Figure 4 displays SEM images of a worn SCD tool used for turning of 15% (volume fraction) SiC_p/2009Al [39].

As can be observed from Fig. 5, the cutting speed, depth of cut, feed rate, and nose radius are the main factors that affect tool wear significantly in most of the turning cases [56]. For instance, the tool wear increases with increasing cutting speed, depth of cut, and feed rate when turning 5%–20% (mass fraction) SiC-reinforced MMCs using an HSS cutting tool [36]. When turning SiC_p/Al7075 MMC with multilayer TiN-coated WC inserts in a dry machining environment, the most significant parameter affecting tool flank wear was cutting speed, followed by feed rate and depth of cut [57].

Based on experiments and modeling of tool deterioration, it is found that the volume fraction of SiC reinforcement strongly influences the tool wear [58]. Higher percentages of SiC particles lead to higher tool wear. A higher surface contact rate between the SiC particles and cutting edge occurs in higher-percentage SiC_p/Al matrix composites [47]. During turning, when the SiC particles gain higher kinetic energy, they will strike the tool insert surface, which causes severe wear [56]. Improving cooling

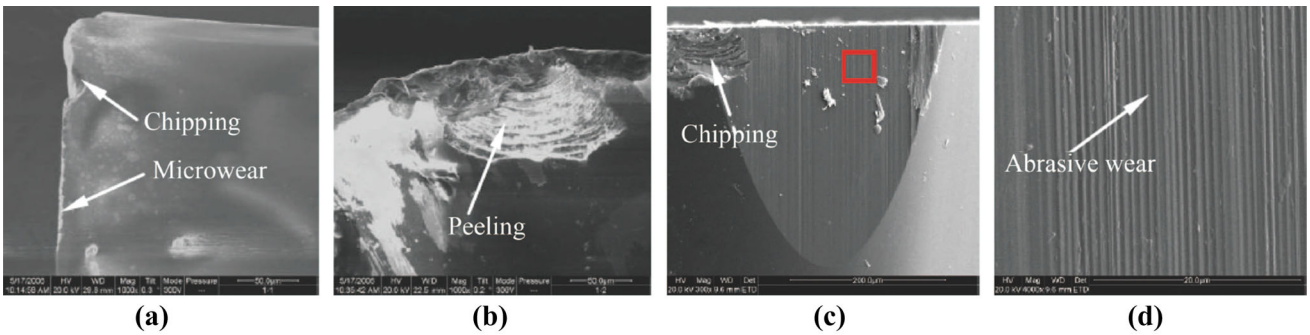

Fig. 4 SEM micrographs of round-edged SCD tool wear after cutting 15% (volume fraction) SiC_p/2009Al: **a** flank face, **b** rake face, **c** flank face on the tool nose and **d** high magnification of the rectangle in **c** [39]

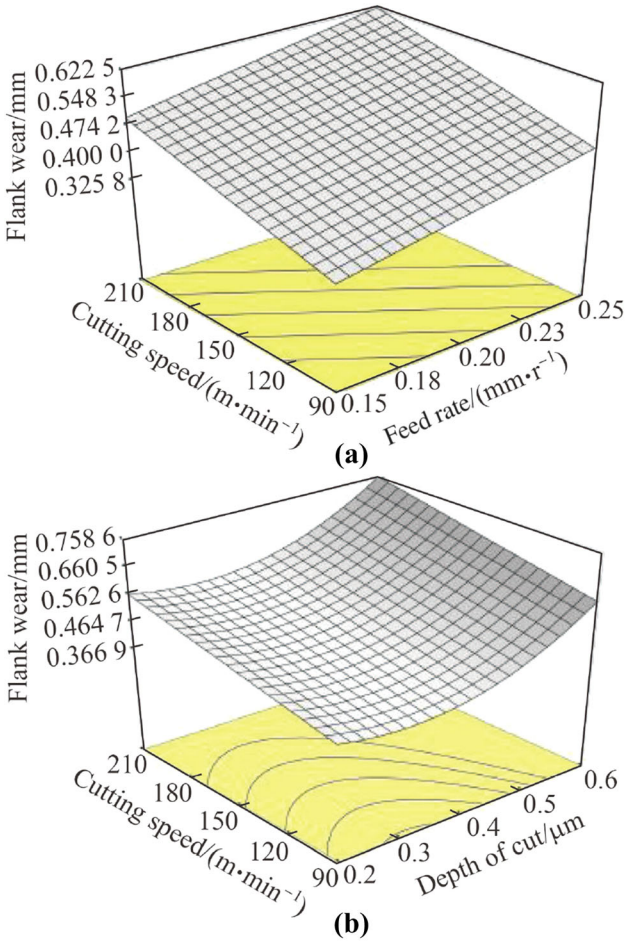

Fig. 5 Effects of **a** cutting speed and feed rate and **b** cutting speed and depth of cut on flank wear [56]

and lubrication has significant impacts on the flank wear, adhesive wear, and tool breakage. It was demonstrated that adequate flushing as well as excellent lubricating and cooling properties would help to reduce the three-body abrasion at the boundary zones of the minor and major flanks [59].

Since tool wear is an important factor that contributes to the variation in spindle motor current, speed, feed rate, and depth of cut, on line tool wear state detecting is available. By analyzing the effects of tool wear and cutting parameters on the current signal, models on the relationship between the current signals and the cutting parameters were established with a partial design taken from experimental data and regression analysis. The fuzzy classification method was used to categorize the tool wear states to facilitate defective tool replacement at the appropriate time [60]. Besides, artificial neural networks (ANNs) and the coactive neuro-fuzzy inference system are available for predicting the flank wear [61].

3.1.3 Cutting force, chip formation, and simulation

The resultant cutting force consists of components due to chip formation, ploughing and particle fracture, and displacement. Merchant's shear plane analysis, slip-line field theory, and Griffith's theory can be adopted for calculating these force components, respectively [62]. Generally, as the cutting forces increase with the flank wear of the turning inserts, the feed and depth forces show a corresponding increase [63]. Manna and Bhattacharayya [54] conducted a series of experiments and found that the cutting force was smaller at lower cutting speeds, whereas the feed force was larger at lower cutting speeds than at higher cutting speeds. Besides, the properties of the SiC particle reinforcement, such as size and volume fraction, contributed to the change in the cutting forces [64]. Gaitonde et al. [65] illustrated that a combination of a high cutting speed with a high feed rate was advantageous for minimizing the specific cutting force. It was demonstrated that the reinforcement percentage had an increasing effect on the resultant force when turning SiC_p/Al composites [66], and the cutting force magnitudes were also sensitive to the size of reinforcement particles [67].

The chips formed from the workpiece material will indicate the material deformation behavior during

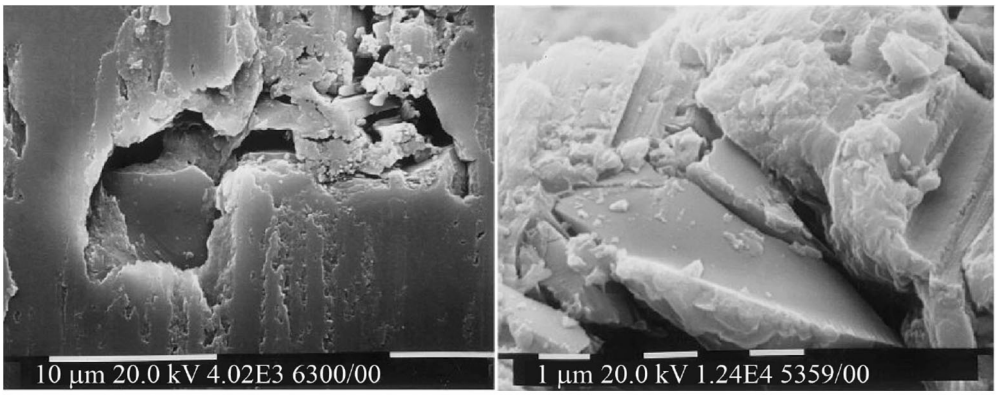

Fig. 6 Surface of the SiC_p/Al chip **a** voids formed around the SiC reinforcements and **b** fractured SiC particles [69]

machining [68]. Figure 6 shows that chip voids initiate around the particles along the inner surface first, and then some SiC particles become fractured [69]. In the turning process, the tool rake angle has a great influence on the chip formation. Normally, the material of the workpiece is removed under the tensile stress supplied by the cutting tool with a positive rake angle. On the contrary, the material is removed under the compressive stress supplied by the cutting tool with a negative rake angle. Therefore, it can be deduced that the plastic deformation of chips occurs more easily when using a tool with a negative rake angle than a tool with a positive rake angle [70].

During turning of SiC_p/Al matrix composites, the primary chip forming mechanism should be the initiation of cracks from the outer free surface of the chip due to the high shear stress [71]. The particles can interfere with matrix plastic deformation and retard the growth of cracks formed in the chip [72]; thus, the size and volume fraction of reinforcement significantly influence the chip formation mechanism. In the case of finer reinforcement composites, the chip segments are longer and gross fracture occurs at the outer surface of the chips only. By contrast, in coarser reinforcement composites, complete gross fracture causes the formation of smaller chip segments [73]. Because the volume fraction of SiC increases the chip disposability, the chip thickness ratio and shear angle increase [53], and the sizes of chips are decreased during dry machining operation [36]. Ge et al. [74] discovered that a saw-toothed chip was formed during ultraprecision turning of SiC_p/Al composites and the chip-formation mechanisms were dynamic microcrack behavior and strain concentration.

Generally, cutting force and chip formation in the turning processes are complex. Simulation models have been developed for a better understanding of these processes. For example, Kishawy et al. [75] reported an energy-based analytical force model for orthogonal cutting of MMCs. Dandekar and Shin [76] proposed a multistep three-dimensional (3D) finite element model using commercial finite element packages to predict the subsurface damage after machining of particle-reinforced MMCs. The particles and matrix were modeled as continuum elements with isotropic properties separated by a layer of cohesive zone elements representing the interfacial layer to simulate the extent of particle-matrix debonding and subsequent subsurface damage. A random particle dispersion algorithm was applied for the random distribution of the particles in the composite. Duan et al. [77] also simulated the chip formation and cutting force in SiC_p/Al composite machining by developing a three-phase friction model that considered the influence of matrix adhesion, two-body abrasion, and three-body rolling. The schematic of the tool-chip interface in SiC_p/Al composites machining is depicted in Fig. 7. It was found that the change in the tool-chip interface friction coefficient with the particle volume fraction and particle size was reasonable. The chip root micrographs obtained from the experiments showed that two-body sliding, three-body rolling, and matrix sticking were the main contact forms that determined the tool-chip interface friction in SiC_p/Al composite machining. As exhibited in Fig. 8, Wu et al. [78] developed a microstructure-based model for investigating the mechanisms of chip formation in the machining of particulate-reinforced MMCs. The morphology and distribution of the particles, debonding of the particle-matrix interface, and fracture of particles and the matrix were comprehensively integrated into the model. Because of the high strain and strain rate throughout the cutting process, the Johnson-Cook (J-C) constitutive model is generally utilized to describe the properties of matrix materials in simulations [79–82]. The J-C equation is based on experimentally determined flow stresses and is a function of strain, temperature, and strain rate in separate multiplicative terms [83]. It is given by

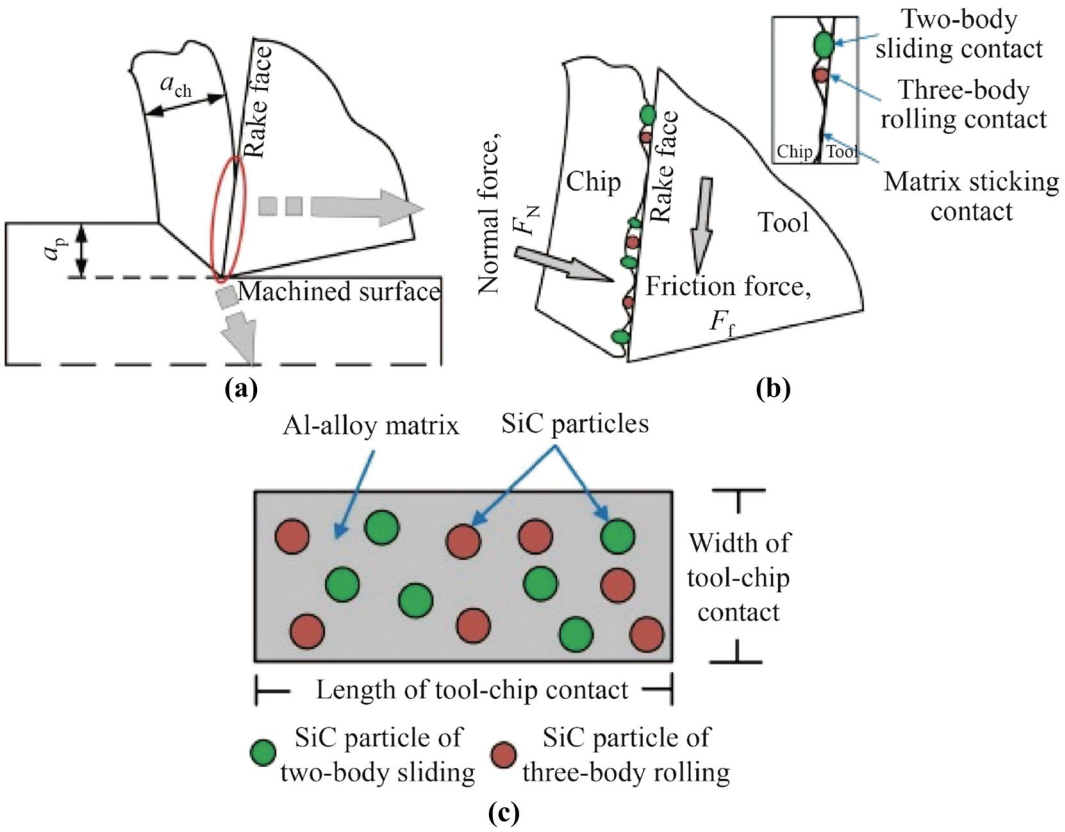

Fig. 7 Schematic of the tool-chip interface in SiC_p/Al composite machining **a** the tool-chip contact, **b** an enlarged view of matrix sticking, two-body sliding, and three-body rolling, **c** an enlarged view of the tool-chip contact face [77]

$$\sigma = (A + B\varepsilon^n)\left(1 + C\ln\left(\frac{\dot{\varepsilon}}{\varepsilon_0}\right)\right)\left(1 - \left(\frac{T - T_r}{T_m - T_r}\right)^m\right),$$

where σ is the flow stress, σ the plastic strain, $\dot{\varepsilon}$ the strain rate, ε_0 the reference plastic rate, T and T_m the current temperature and material melting temperature, respectively, T_r the room temperature, A, B, C, n, and m the material constants that can be obtained using dynamic Hopkinson bar tensile tests. In some conditions, e.g., if the strain exceeds a certain value (0.3) or under a high strain rate condition (higher than 10^3/s), a modified J-C constitutive model with a correction of strain and strain rate hardening is used for the simulation of turning of particle-reinforced MMCs [78]. A detailed summary of machining models for composite materials can be found in Ref. [84].

3.1.4 Surface integrity and machining efficiency

With turning, the machined surfaces contain many defects of pits, voids, microcracks, grooves, protuberances, matrix tearing, and so on [85]. In investigations on the machining surface roughness (SR), R_a (the arithmetic mean roughness), R_t (the maximum peak-to-valley height of roughness) [86], and R_z (the maximum peak-to-valley height within sampling length) [87] are generally considered. Ding et al. [88] studied the machining performance of SiC_p/Al composites with various types of polycrystalline CBN and PCD tools; they explained that the adhesion property of the tool and the work material had a major influence on the surface finish. Sharma [89] studied the interaction effects of various factors and reported that an increase in nose radius improved the SR, while the feed rate has a more severe effect on the SR. Davim [90] proposed that the cutting velocity, cutting time, and feed parameters had statistical and physical significance on the SR of the workpiece. Palanikumar and Karthikeyan [91] insisted that feed rate was the main factor that had the greatest influence on the SR, followed by the cutting speed and SiC volume fraction. Muthukrishnan and Davim [92] also supported that the feed rate has the highest statistical and physical influences on the SR, whereas Manna and Bhattacharayya [48] considered that the cutting speed, feed rate, and depth of cut had equal influences on the R_a and R_t values. Aurich et al. [93] suggested that high cutting speeds and feed rates and moderate depths of cut needed to be used to decrease the thermal load of the workpiece. Muthukrishnan et al. [35] found that the surface finish was superior at lower feed rates and higher cutting speeds for

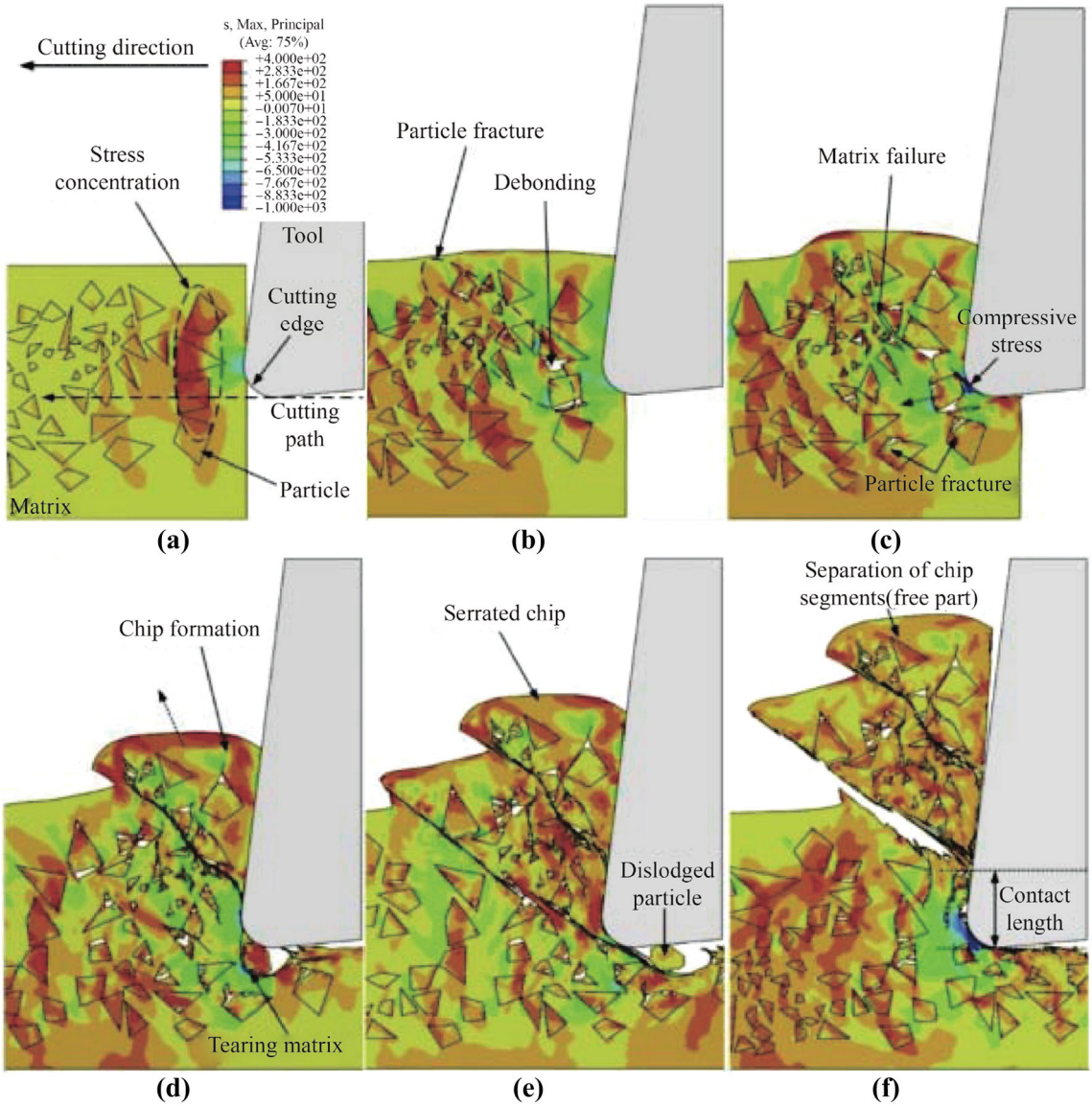

Fig. 8 Simulations of distribution of principal stress under a 50 μm depth of cut [78]

PCD inserts. When the cutting speed was 400 m/min, a steady low R_a value could be obtained over the entire tool life, which made high-speed finishing of MMCs possible [94]. Ge et al. [95] reported that R_a of 20–30 nm could be attained by using single-point diamond tools (SPDT) or PCD tools; moreover, the surface obtained by SPDT was smoother and the number of crushed or pulled out SiC particles was fewer. Dabade et al. [96] observed the lowest SR (R_a = 0.13 um) on the machined surfaces of higher-fraction reinforced MMCs (Al/SiC/30p), and the maximum SR (R_a = 2.47 μm) was found on the machined surfaces of Al/SiC/20p composites. It was reported that the SR of the cutting surface decreased as the volume fraction of SiC decreased [97], and the change in size was more influential than the volume fraction [96]. Wang et al. [98] conducted precision turning experiments to study the influence of particle size on the surface quality and proved that the SR (peak-valley value) was close to the particle radius. The performance of cutting tool materials has been evaluated in terms of surface quality from the best to the worst, which are PCD, CBN, and WC (for 10%(mass fraction) SiC_p/Al) [99]. For example, while turning Al2124-SiC (45%(mass fraction)) MMCs, the PCD tool performed better than the CBN tool with lower flank wear and higher surface finish quality [100]. It was proposed that damage to the machined surface was related to the fracture and pluck out of SiC reinforcement by cutting tools [101]; specifically, the particles beneath the machined surface were fractured as subsurface damages because of squeezing by the flank face of the cutting edge [78]. Hence, the treated tool produces a

better-machined surface of MMC material than the untreated tool [102], and lubrication will be helpful. In particular, kerosene with graphite powder yields better results on SR and surface hardness compared with other lubricants such as soluble oil, mineral oil, and pure kerosene [103]. In general, the peak residual stresses and residual stresses at most depths beneath the machined surface are higher for heat-treated samples than those for hot-rolled samples [104]. Concerning investigations conducted by Aurich et al. [105], the use of high feed rates decreased the residual stress in the surface of the workpiece in comparison to using low feed rates. However, the surface quality considerably deteriorated by using high feed rates. As depicted in Fig. 9, Sharma [89] studied the interaction effects of various factors and reported that an increase in nose radius improved the SR while the feed rate had a more severe effect on the SR, which increased with the increase in feed rate.

Machining efficiency is an important factor in the machining operation of SiC_p/Al composites. The operational cost of the machine is directly proportional to the square of the material removal rate (MRR) [56]. MRR is determined by the rate of change in volume [106]. In the turning process, the value of MRR (r_{MRR}) is calculated by the following formula: $r_{MRR} = V \times F \times D$. Here, V is the cutting speed (m/min), F the feed rate (mm/r), and D the depth of cut (mm). Theoretically, increasing any of V, F, or D will significantly improve the machining efficiency.

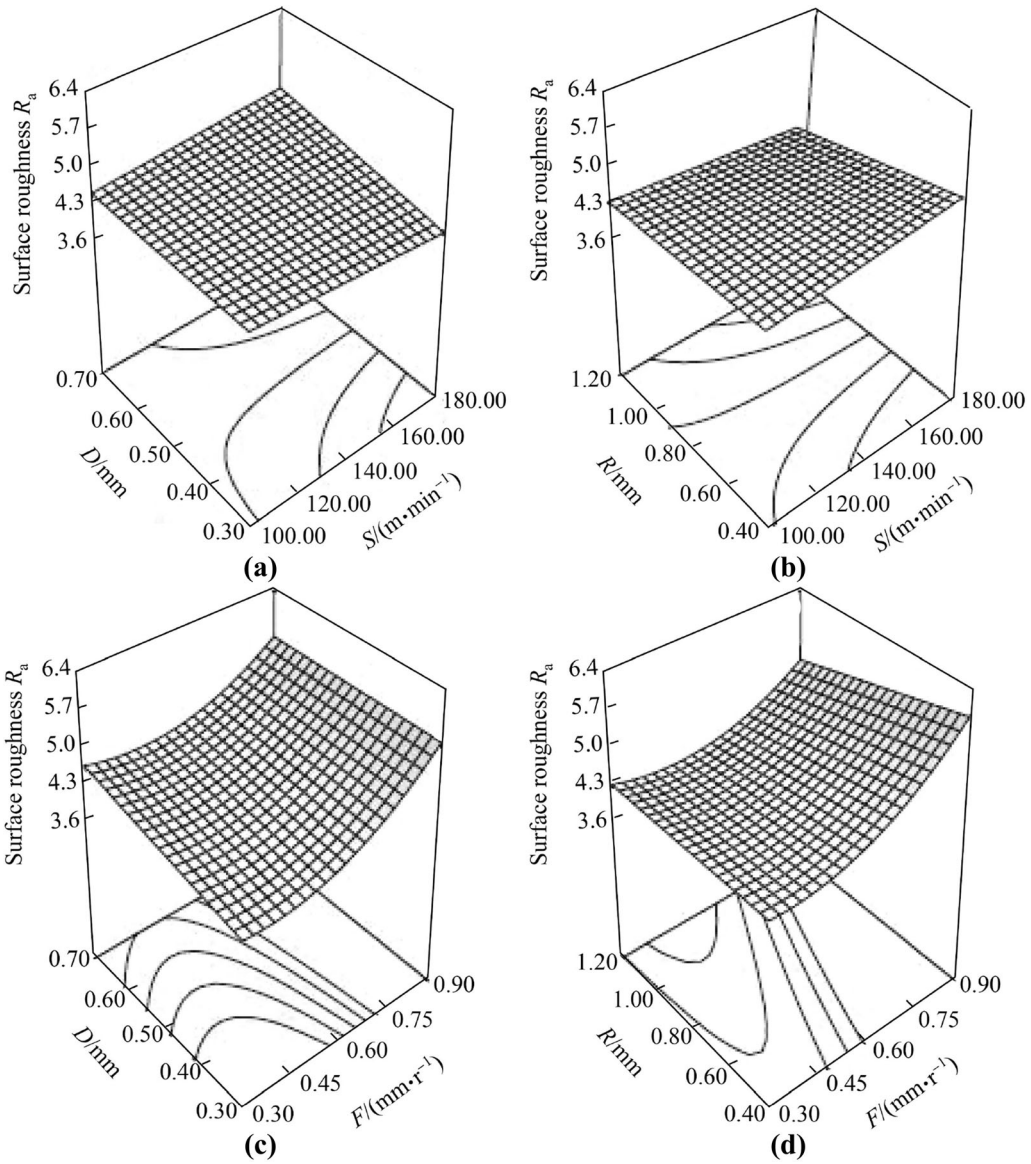

Fig. 9 Interaction effects of various factors on surface roughness (S: cutting speed, D: depth of cut, F: feed rate, and R: nose radius) **a** cutting speed versus depth of cut, **b** cutting speed versus nose radius, **c** depth of cut versus feed rate, and **d** feed rate versus nose radius [89]

However, the change in cutting parameters will produce non-negligible influences on other aspects, e.g., tool life, cutting force, energy consumption, and surface quality. Thus, it is necessary to optimize the machining parameters to achieve higher efficiency without causing severe tool wear, large energy consumption, etc. Generally, optimization methods, e.g., ANOVA and gray relational analysis [56, 107, 108], genetic algorithms (GAs) [109], Taguchi's optimization methodology [110–114], and response surface methodology (RSM) [115–118], have been adopted. Table 1 lists various recommended turning parameters for industry consideration based on optimization studies from Refs. [119–124].

Table 1 Recommended turning parameters for industry

Tool	Matrix	SiC fraction	Parameter	Remark
PCD [119]	Al 356	5% (mass fraction)	Spindle speed 1200 r/min, feed rate 0.25 mm/r, depth of cut 1.0 mm	Surface roughness 2.96 μm, r_{MRR} 37.79 cm^3/min
HSS [120]	Al 7075	10% (mass fraction)	Feed rate range of 0.4–0.8 mm/r, depth of cut range 0.08–0.16 mm, cutting speed range of 60–100 m/min	Cutting forces are independent of cutting speed
Carbide insert [121]	Al 7075	10% (mass fraction)	Cutting speed range of 180–220 m/min, feed rate range of 0.1–0.3 mm/r, and depth of cut range of 0.5–1.5 mm	Optimum surface oughness
PCD [122]	Al 7075	10% (mass fraction)	Low feed rate (0.05 mm/r) and high cutting speed (170 m/min)	The best surface finish
Carbide insert [123]	Al 7075	15% (mass fraction)	Cutting speed 90 m/min, feed rate 0.15 mm/r, depth of cut 0.20 mm, nose radius 0.42 mm	The maximum value of tool life (6.6 min)
K20 series [124]	Al 6025	20% (volume fraction)	Narrow region around 150 °C and 150 m/min as the optimum domain for machining	Tool: a thick Al_2O_3 layer on top of Ti(C,N) layer

3.2 Milling

There are several types of milling methods, e.g., end milling and face milling. From an overview of the literature, it can be found that most investigations of SiC_p/Al composite machining are focused on end milling.

3.2.1 Tool wear

Uncoated cemented carbide inserts, nano TiAlN coated tools, and carbide-coated cutting tools can be adopted for the milling of SiC_p/Al composites. Additionally, some ultrahard materials, such as CBN and PCD, are employed to avoid rapid tool wear [125]. Images of a milling cutter with an identical tool geometry are exhibited in Fig. 10 [126].

Shen et al. [127] demonstrated that the uncoated WC-Co milling tool sufferred the severest wear in its circumferential cutting edge, whereas the wear of the diamond-like carbon (DLC)-coated milling tool was slightly lower. Comparatively, the CVD diamond-coated milling tool exhibits a much stronger wear resistance. The wear on its circumferential cutting edge is less than 0.07 mm at the end of milling tests, which is only half of that of the DLC-coated milling tool. Huang et al. [128] conducted high-speed milling experiments of SiC_p/Al composites with 20% (volume fraction) at dry and wet machining conditions. The results showed that the main tool wear was abrasion on the flank face, and the TiC-based cermet tool was not suitable for machining SiC_p/Al composites with higher volume fractions and larger particles due to the heavy abrasive nature of the reinforcement. The diamond particle size has a great influence on the wear resistance of PCD tools. The larger the size of the diamond particle, the worse the wear resistance. However, when the tool wear goes into a stable wear state, the wear rate of PCD tools with different particle sizes is almost the same [129]. Wang et al. [130] showed that the wear pattern of PCD tools was the flank wear caused by abrasion of the SiC particles at relatively low cutting speeds. Since graphitization of PCD tools does not occur at low cutting temperatures, the wear mechanism of PCD tools will be abrasive and adhesive wear. Huang and Zhou [131] also reported that the flank wear was the dominant wear mode for the TiN-coated tool, cermet tool, and cemented carbide tool. The wear resistance was almost the same for the three different tool materials at both low and high speeds. In addition, the milling speed was the most influential machining parameter on tool wear. With increasing milling speed, the tool wear increased. The feed rate and depth of cut have slight influences on the tool wear. As shown in Fig. 11, Ge et al. [132] reported the tool flank wear under different working times during high-speed milling of a SiC/2009Al composite using a PCD tool; the

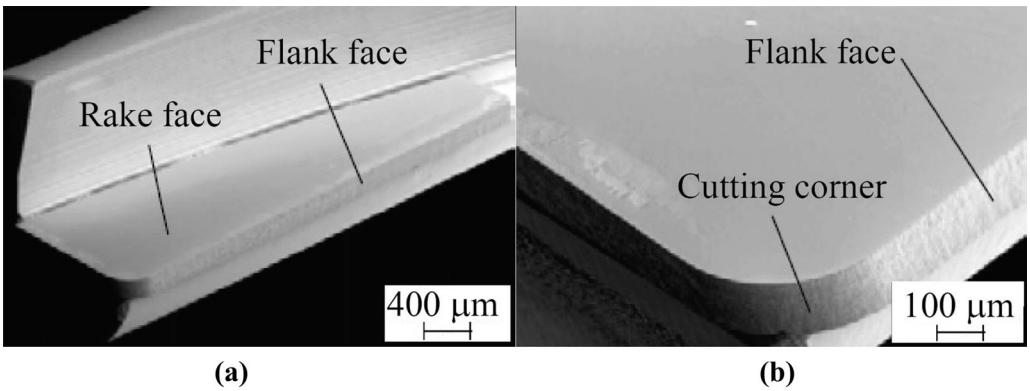

Fig. 10 Milling cutter geometry: **a** tool faces and **b** cutting corner [126]

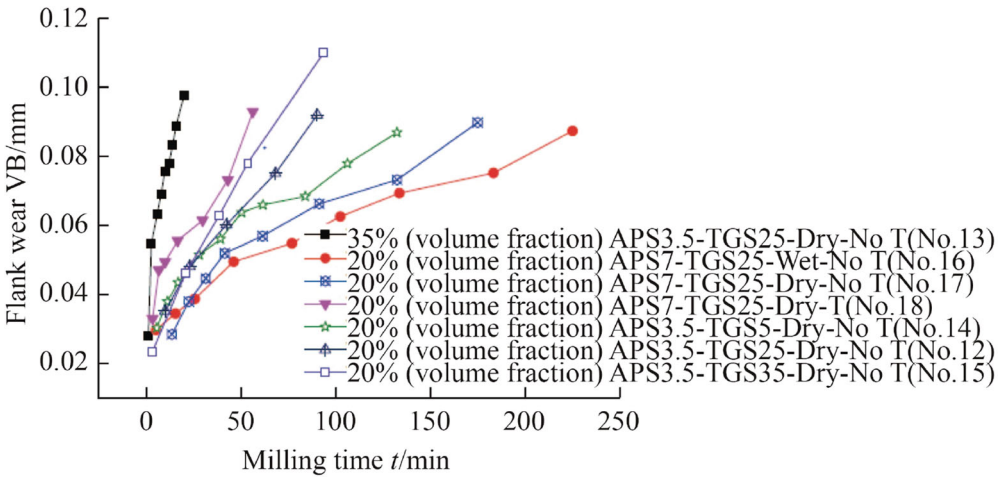

Fig. 11 PCD tool life comparison under different milling conditions [132]

available tool life could exceed 240 min when a 0.1 mm tool wear criterion was chosen. It was reported that the wear mechanism of diamond-coated micromills was adhesion, abrasion, oxidization, chipping, and tipping [133], and the volume fraction and size of SiC particles present in the aluminum alloy matrix had significant effects on the milling characteristics [134, 135].

3.2.2 Cutting force

The cutting force and its impact factors in different milling investigations are generally not the same; however, the machining parameters and SiC particles play a key role.

Jayakumar et al. [136] revealed that the depth of cut and size of SiC were the key impact factors of the cutting force. An increase in the volume fraction of SiC reinforcement over the matrix results in a higher tool-work interface temperature and requires a higher cutting force [137]. Vallavi et al. [138] observed that the cutting speed had negative effects on the cutting force while the axial depth of cut and the percentage of SiC showed positive effects on the cutting force. Huang et al. [139] also detected that the milling forces decreased with an increase in the milling speed, or increased with an increase in the feed rate and depth of milling. The influence of milling depth on the milling forces in the x and y directions is the most significant, while the influence of the feed rate on the z milling forces is the most significant. Babu et al. [140] demonstrated that the cutting force components were more sensitive in the high-speed and full immersion condition, and it was witnessed that the cutting force obtained additional undulations by both the unstable chip formation of composite material and randomly distributed reinforcement particles [141].

Ge et al. [142] performed high-speed milling tests on SiC_p/2009Al composites by using PCD tools in the speed range of 600–1 200 m/min. The results showed that the peak value of the cutting force (in the tool radial direction) was in the range of 700–1 450 N. The maximum amplitude of the cutting force vibration in the tool radial direction can reach 700 N. Figure 12 illustrates the cutting forces and torque in high-speed milling of SiC_p/Al composites with

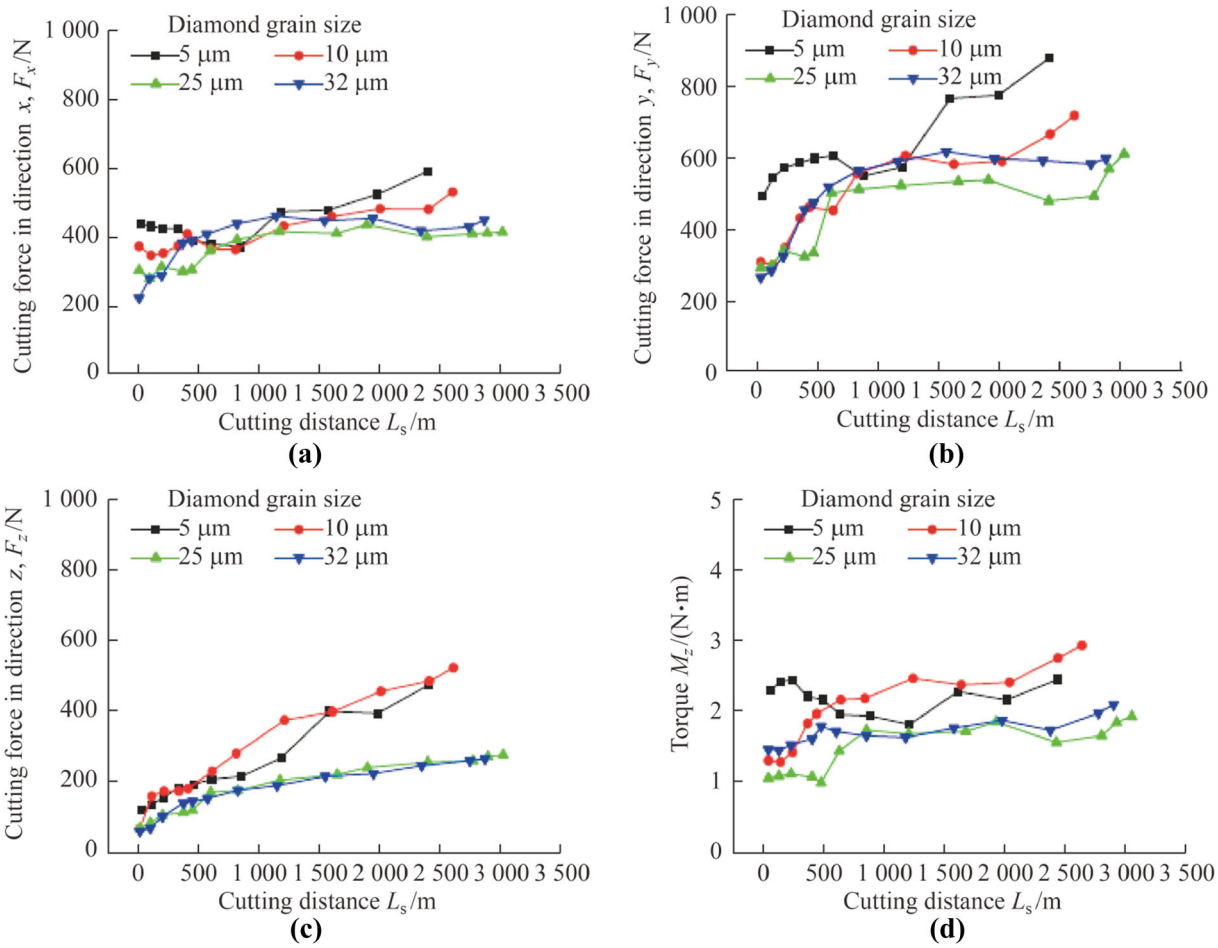

Fig. 12 Cutting force versus cutting distance **a** F_x, **b** F_y, **c** F_z and **d** torque [143]

small particles and high-volume fraction by adopting PCD cutters with different grain sizes [143]. The cutting forces and torque of PCD tools of larger diamond grain sizes are less than those of smaller diamond grain sizes.

3.2.3 Surface integrity, machining efficiency, and optimization

The SiC reinforcement removal mode plays a decisive role in the formation of the machined workpiece surface [144]. Various defects concerning surface topography such as ploughed furrow, pits, and matrix tearing have been found under different parameters, which are mainly the effect of SiC particles pulled out, fractured, or crushed [145]. Figure 13 depicts the machined surface morphology of Al6063/SiC_p/65p composites. The machined surfaces are characterized by shallow pits caused by fractured or crushed SiC particulates, swelling formed by pressed-in SiC particulates, large cavities formed from pulled-out SiC particulates, and high-frequency scratches of SiC particulates.

The reinforcement enhances the machinability in terms of both SR and lower tendency to clog the cutting tool compared to a non-reinforced Al alloy using TiAlN-coated carbide end mill cutters [146]. Zhang et al. [147] reported that the SR of aluminum/SiC composites was smaller than that of the aluminum metal during an end milling experiment, which was due to the improvement in mechanical properties of the aluminum/SiC composite resulting from the addition of SiC particles. In the precision milling of the composites, the generation of the machined surface is a balance between the size effect of the Al matrix and the removal methods of SiC particles. When the feed per tooth is smaller than the minimum chip thickness of Al, the coating effect is dominant; when the feed per tooth is larger than the maximal advised value calculated by the method, the particle cracks dominate [148]. The SR mainly depends on the feed rate followed by the spindle speed, whereas the depth of cut has the least influence [149]. Thus, high cutting speeds, low feed rates, and low depths of cut are recommended for better surface finish [150]. Obtaining a very smooth surface for a high-volume fraction and large

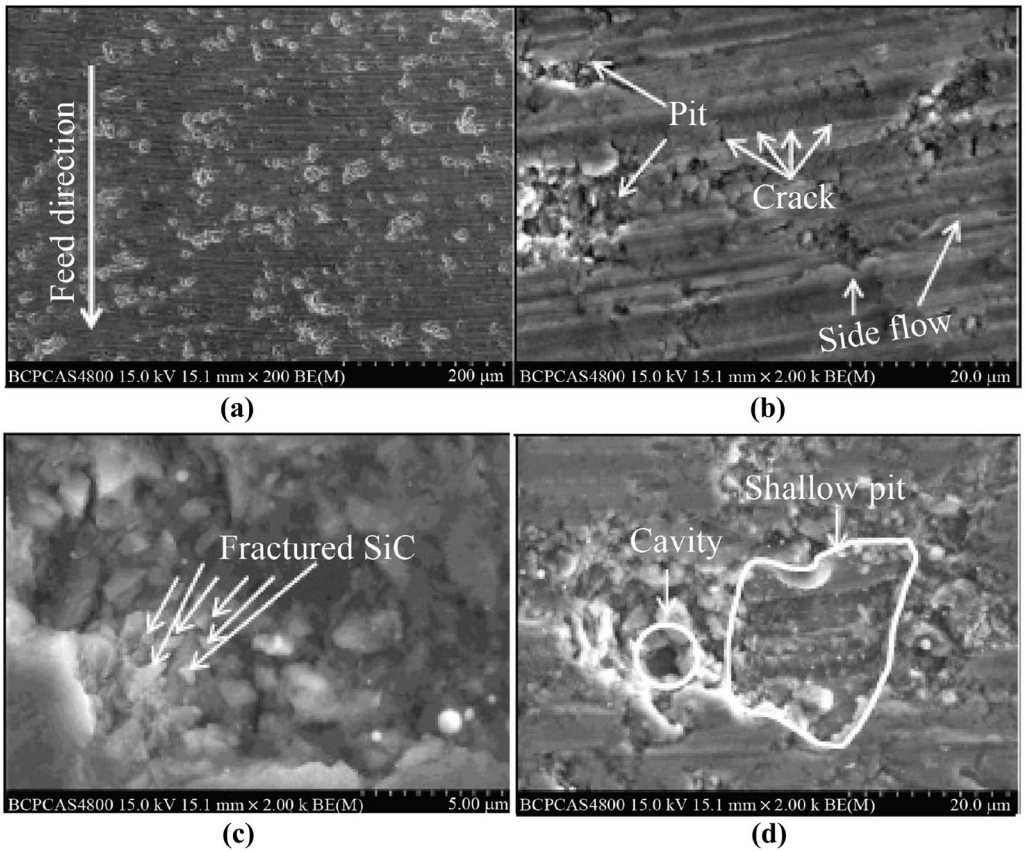

Fig. 13 SEM micrographs of the Al6063/SiC_p/65p machined surface **a** macromachined morphology, **b** scratch and microcrack, **c** cavity formed by SiC cracking, **d** shallow pit caused by SiC scratch, **e** cavity formed by pulled-out SiC particulate and **f** swelling caused by pressed-in SiC particulate [6]

SiC particle workpiece is very difficult; however, a mirror-like surface with an SR (R_a) of approximately 0.1 μm can still be achieved by using diamond precision milling with small parameters in the range of a few micrometers [125].

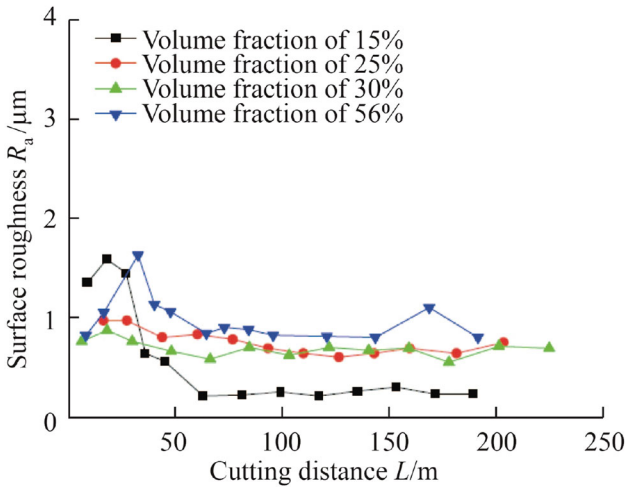

Fig. 14 Relation curves between cutting distance and machined surface roughness (using PCD tools) [153]

Wang et al. [151] reported that the milled SR of 65% (volume fraction) SiC_p/Al composites decreases gradually when the milling speed increases from 100 m/min to 250 m/min, and then the values remain stable. It has been demonstrated that using a CO_2 cryogenic coolant can improve the surface quality by reducing the SR value (in face milling) [152]. Figure 14 indicates the influence of SiC fraction on the SR [153]. When the machined SR enters into a relatively stable state, the SR of machined materials with a volume fraction of 56% is the highest, and the value is the lowest when the volume fraction of SiC particles is 15%. When the volume fractions are 25% and 30%, the values of the machined SR have little difference between each other. In general, the lower the volume fraction of SiC particles, the smaller the machined SR.

In terms of residual stress on the machined surface, the axial depth of cut has the highest influence, followed by the milling speed and feed rate, and the residual stress measured in the feed direction indicated that the conditions of the machined Al6063 surface were all tensile, while the conditions of Al/SiC/65p were compressive [154]. During milling, the matrix material was removed in a plastic way

Table 2 Recommended parameters for the milling of SiC_p/Al composites

Tool	Matrix	SiC (volume fraction)	Parameter	Remark
End mill cutter (ϕ 16 mm) with 2 uncoated cemented carbide inserts [136]	A356 aluminium alloy	10%	Cutting speed 200 m/min, feed rate 0.1 mm/min, depth of cut 0.2 mm	The minimal surface roughness and cutting forces
Three different cutting tools (uncoated, multi-layered and nano TiAlN coated) [135]	123 L aluminium alloy	10% SiC under 32 μm	Uncoated tool: cutting speed 60 m/min, feed rate 0.04 mm/r; multi-layered tool: cutting speed 78 m/min, feed rate 0.12 mm/r	Multi-layered tool 0.302 μm
Carbide insert with a 0.8 mm uncoated tool nose radius [160]	Al7075 alloy	40%	Cutting speed 170 m/min, depth of cut 0.8 mm and a feed per tooth 0.08 mm/tooth.	Best surface quality
Carbide coated cutting tool inserts (AXMT 0903 PER-EML TT8020) [43]	Al7075 alloy	5%, 10%, 15%	Spindle speed 1000 r/min, feed 0.03 mm/r, depth of cut 1 mm and 5% SiC by weight	The best combination
PCD blade with carbide substrate [161]	Al6063 aluminum	65%	Cutting speed 300 m/min with a tool refreshment	Surface R_a less than 0.4 μm

and presented a smooth machined surface. Most of the SiC reinforcements presented partial ductile removal with microfractures and cracks on the machined surface [125]. The material removal and tool wear mechanism in the milling of SiC_p/Al composites are complex. Investigations aimed at achieving a higher MRR, lower tool wear, and higher surface quality have been conducted; thus, RSM [155–157], gray-fuzzy logic algorithm [158], and ANOVA [159] have been adopted. Based on the literature, the recommended milling parameters for industry application are listed in Table 2 [43, 135, 136, 160, 161].

3.3 Drilling

Solid carbide drills, TiN-coated HSS twist drills, PCD-coated drills, and CVD diamond-coated carbide tools are widely used for the drilling process. Tosun and Muratoglu [162] advised that solid carbide drills were the most suitable tools for drilling of 17% (volume fraction) SiC_p/Al composites, however, from an estimate of economic factors, the TiN-coated HSS drills were cheaper than the solid carbide tools. The best performance of the TiN-coated HSS twist drill was obtained with a lower cutting point, higher feed rate, and higher cutting speed [163]. Xiang et al. [41] suggested that when drilling high-volume fraction (e.g., 65%(volume fraction)) SiC_p/Al composites, the CVD diamond-coated carbide tool should be preferred, owing to its stable cutting force, less tool wear, and its ability to produce acceptable machining quality. Monaghan and O'reilly [164] compared a series of drilling tests on a 25% (volume fraction) SiC/Al composite with different drilling tools (coated and uncoated HSS, carbide and PCD-tipped drills, and solid-carbide drills). The results indicated that the hardness of the tool material had a significant influence on the machining performance, and the presence of a ceramic coating on an HSS drill did not improve its performance appreciably compared to standard uncoated tools.

The height of burrs produced during drilling was found to be greater with softer materials [165]. Moreover, burr dimensions were smaller at a lower feed rate, higher point angle, and higher concentration of reinforcements [166]. The experiment conducted by Babu et al. [167] showed that the point angle had a significant influence on the drilling performance. As the point angles of HSS and TiN-coated HSS drills increase, the damage zone increases. However, with increasing point angles of solid carbide drills, the damage zone decreases [168]. The temperature during the cutting process plays a major role in the tool wear evolution and wear mechanism [169, 170]. The heat generation during machining is divided into plastic-deformation heat and friction-induced heat. The converted heat rate by plastic deformation leads to workpiece temperature variation in material forming and machining. Figure 15 shows the schematic of heat partitioning in the chip formation process.

Huang et al. [171] reported that the thrust force varied linearly with the feed rate, while the cutting speed had no significant effect on the thrust force when drilling SiC_p/Al composites with high-volume fractions (55%–57% SiC) and large particle sizes. Hu et al. [172] developed a 3D finite element model for simulating the 3 mm diameter peck drilling behavior of SiC_p/Al composites by using ABAQUS/Explicit. In the simulation, a J-C model was created for the SiC_p/Al composites. A comparison of the simulation and experimental chip formation is shown in Fig. 16.

As displayed in Fig. 17, many uniform and close-packed abrasion marks on the chisel edge and flank face can be

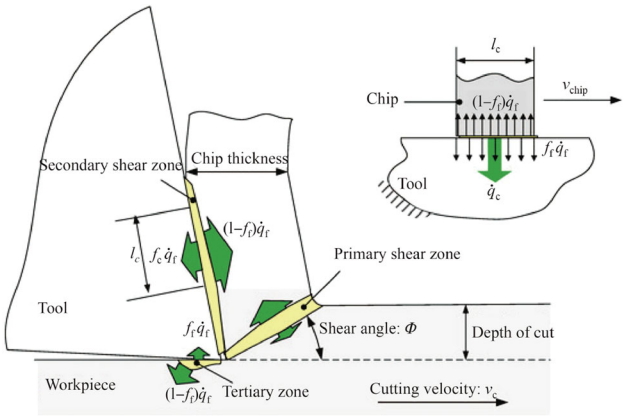

Fig. 15 Schematic of heat partitioning in the chip formation process [170]

observed when drilling SiC_p/Al composites with high-volume fractions and large SiC particle sizes using electroplated diamond drills [173]. It can be seen that the wear of the embedded diamond grit on the drill includes abrasive wear (see Fig. 17a), pullout (see Fig. 17b), cracks initiated around the particle (see Fig. 17c), and fracture (see Fig. 17d).

Tosun [174] observed that the most influential parameters on the workpiece SR were the drill type and feed rate, respectively. The spindle speed, drill point angle, and heat treatment have been determined to be insignificant factors on the SR. Barnes and Pashby [175] provided strong evidence that through-tool cooling led to a significant improvement in performance in terms of tool wear, cutting force, surface finish, and height of burrs produced. There is another drilling process called friction drilling, which has been adopted for SiC_p/Al matrix composites; it is reported that the hole quality in terms of roundness is affected by the spindle speed, feed rate, and percentage of SiC in the workpiece [176, 177]. Currently, optimization methods are available based on gray relational analysis [178], fuzzy logic and GAs [179, 180], Taguchi's method [181], etc. The recommended drilling parameters for industry consideration are provided in Table 3 [168, 174, 178, 179, 181–183].

3.4 Grinding

Grinding can be performed as surface, cylindrical, and ductile-regime grinding. Among them, cylindrical grinding has attracted most of the research interests in the grinding of SiC_p/Al matrix composites.

3.4.1 Surface grinding

The material removal of SiC particles is primarily due to the failure of the interface between the reinforcement and matrix, and results from microcracks along the interface and many fractures or crushed SiC particles on the ground surface [184]. The chips can be divided into Al-matrix chips, SiC particle chips, and Al-SiC mixed chips, when diamond grinding SiC_p/Al composites with higher volume fraction and larger particles [185]. The grindability is influenced by both the type of grinding wheel abrasive and the type of reinforcement of workpiece material [186]. Zhang et al. [187] compared the PCD compact (PDC) whisker with the CVD diamond whisker, and found that the PDC wheel had better edge evenness, which led to good machining quality. Xu et al. [188] suggested the potential of using SiC wheels for rough grinding of SiC_p/Al composites in consideration of their economic advantages. Zhong [189] reported that there was almost no subsurface damage except for rare cracked particles when fine grinding 10% (volume fraction) SiC_p/Al composites with a diamond wheel. Huang et al. [129] revealed that the normal grinding forces of SiC_p/Al composites were always higher than the tangential grinding forces. With the increase in the grinding depth and table speed, both the normal and

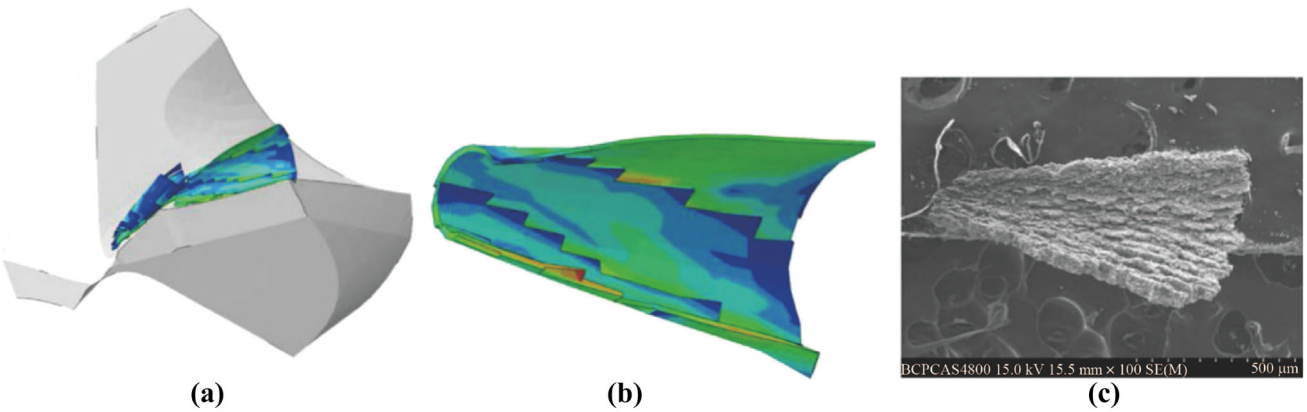

Fig. 16 Chip formation in simulation and experiment: **a** formation of two chip segments, **b** segment B in simulation, **c** segment B in experiment [172]

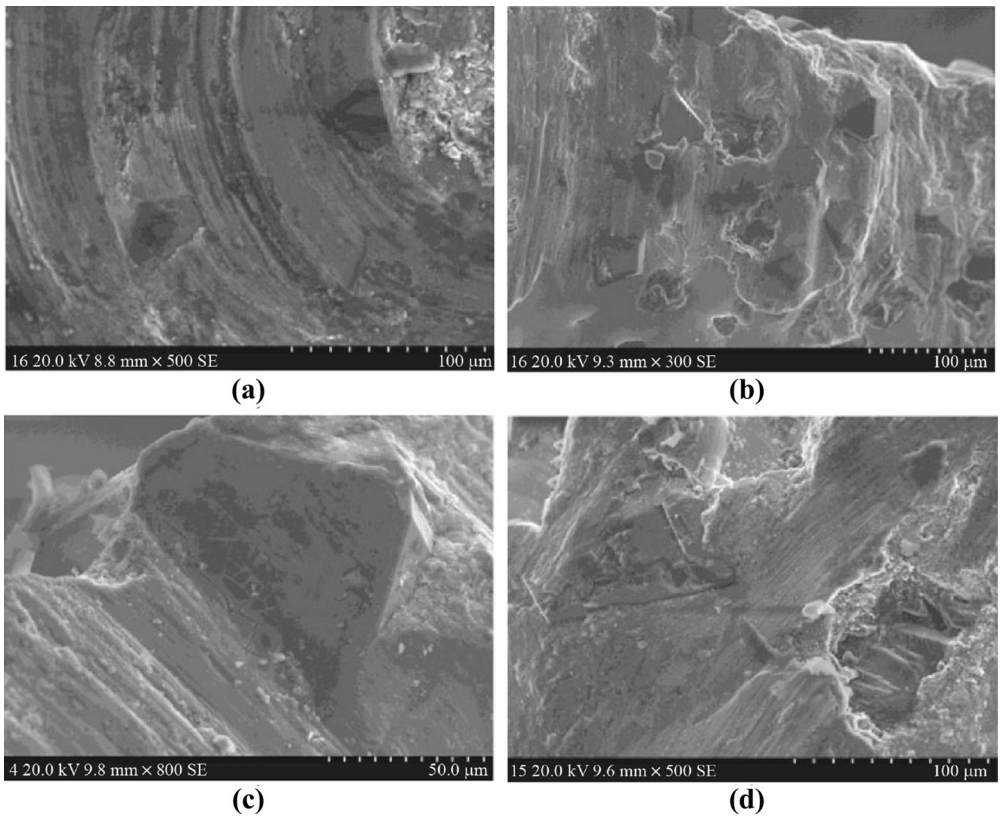

Fig. 17 SEM image of worn diamond grits **a** abrasive wear, **b** pullout, **c** crack initiation and **d** fracture [173]

tangential grinding forces of SiC_p/Al composites increased evidently. Due to the high hardness of SiC_p/Al composites, the thrust component of the grinding force showed a strongly increasing trend with wheel degradation [190]. Furthermore, with an increase in the grinding depth, both the normal grinding force and tangential grinding force increased evidently [191].

Among the different grinding wheels, the diamond wheel exhibits the lowest normal force followed by the CBN wheel. Surface damages such as debonding of reinforcement from the metal matrix cracked reinforcement, particle breakage, and cracks at the surface are the reason for the increased forces while grinding using the SiC wheel [192]. Considering the plastic deformation force of the matrix material, the friction force between grits and workpiece material, and the removal force of SiC particles, a grinding force model suitable for grinding holes of SiC_p/Al composites with high-volume fractions was established by Lu et al. [193]. The effect of the grinding parameters on the grinding force, as shown in Fig. 18, was investigated by Xu et al. [188]. The results indicated that the grinding depth had a more significant effect on the grinding force than the feed speed; with increasing grinding depth and table feed speed, the grinding forces for both the tangential and normal components increased, and the increasing trend was more notable with a higher grinding depth.

The grinding temperature increases with an increase in the wheel velocity, workpiece velocity, feed rate, and depth of cut. High values of the grinding parameters result in high grinding temperatures due to the increase in the energy required to grind a unit volume of material [194]. When the grinding temperature exceeds 450 °C, a black color appears on the ground surface due to the oxidation reaction, and the residual compressive stress of the burned surface layer is very high [195]. By adopting a triangular heat source model, the temperature distribution in the workpiece can be accurately and efficiently calculated during the precision grinding of SiC_p/Al composites [196]. Du et al. [197] established a microgrinding model of SiC_p/Al composites, which took into account the SiC-reinforced particle irregularity, as shown in Fig. 19, and the model was used to analyze the particle removal and surface formation processes in different machining conditions.

In the grinding of SiC_p/Al composites, a common problem is the formation of voids and delamination on the machined surface, which is due to pulled-out reinforced particles and aluminum matrix adhesion on the machined surface. The surface feature of the workpiece varies with different grinding parameters. With a larger feeding

Table 3 Recommended drilling parameters for SiC_p/Al composites

Drill	Matrix	Fraction	Parameter	Remark
8 mm-KISTLER [178]	Al6063	10%	Spindle speed 560 r/min, feed 0.05 mm/r, point angle 90°	Torque and SR were considered as quality targets
5 mm-solid carbide [174]	Al 2124	17%(volume fraction)	Feed rate 0.16 mm/r, spindle speed 260 r/min, drill point angle 130°	The minimum surface roughness obtained
12 mm-HSS [181]	Al6063	15%	Cutting speed of 150.72 m/min, feed rate of 0.05 mm/r	Cutting environment water, soluble oil
5 mm-solid carbide [168]	Al 2124	17%(volume fraction)	Point angles 130, spindle speed 1 330 r/min, feed rate 0.16 mm/r	Carbide tool better that HSS and TiN coated HSS
10 mm-solid carbide [179]	LM25	15%(volume fraction)	Spindle speed 921.0 r/min, feed rate 0.258 mm/r	Metal emoval rate 5 579 mm^3 /min, surface roughness 8.50 μm
3 mm-HSS [182]	Al123	10%(mass fraction)	Cutting speed 20 m/min, feed rate 0.04 mm/r	Cryogenic treatment has positive effects on R_a
5 mm-PCD [183]	A356/	20%	Cutting speed 50 m/s, feed 0.05 mm/r	PCD tool is perfectly compatible with cutting conditions

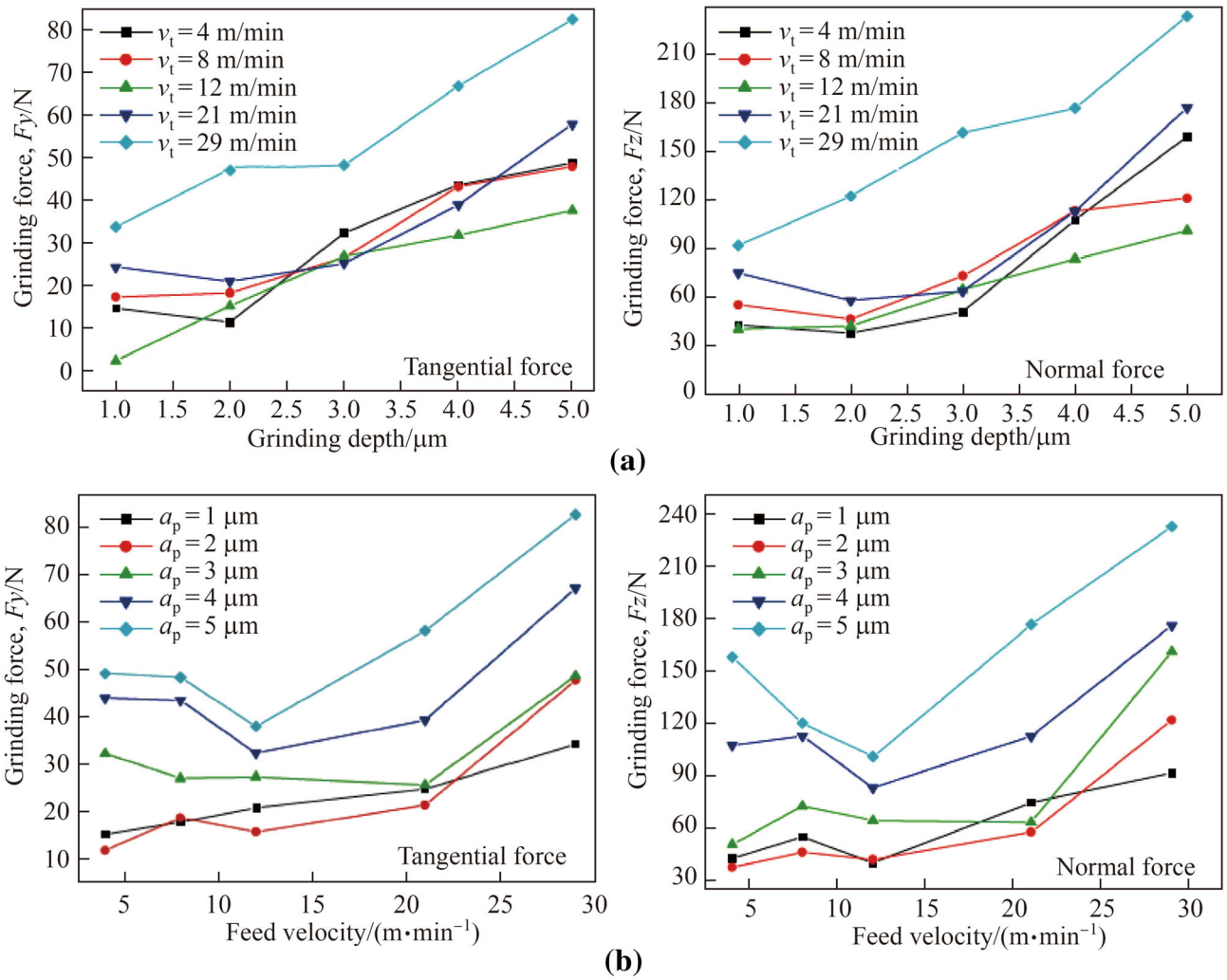

Fig. 18 Typical variation in grinding force with **a** grinding depth and **b** feed velocity [188]

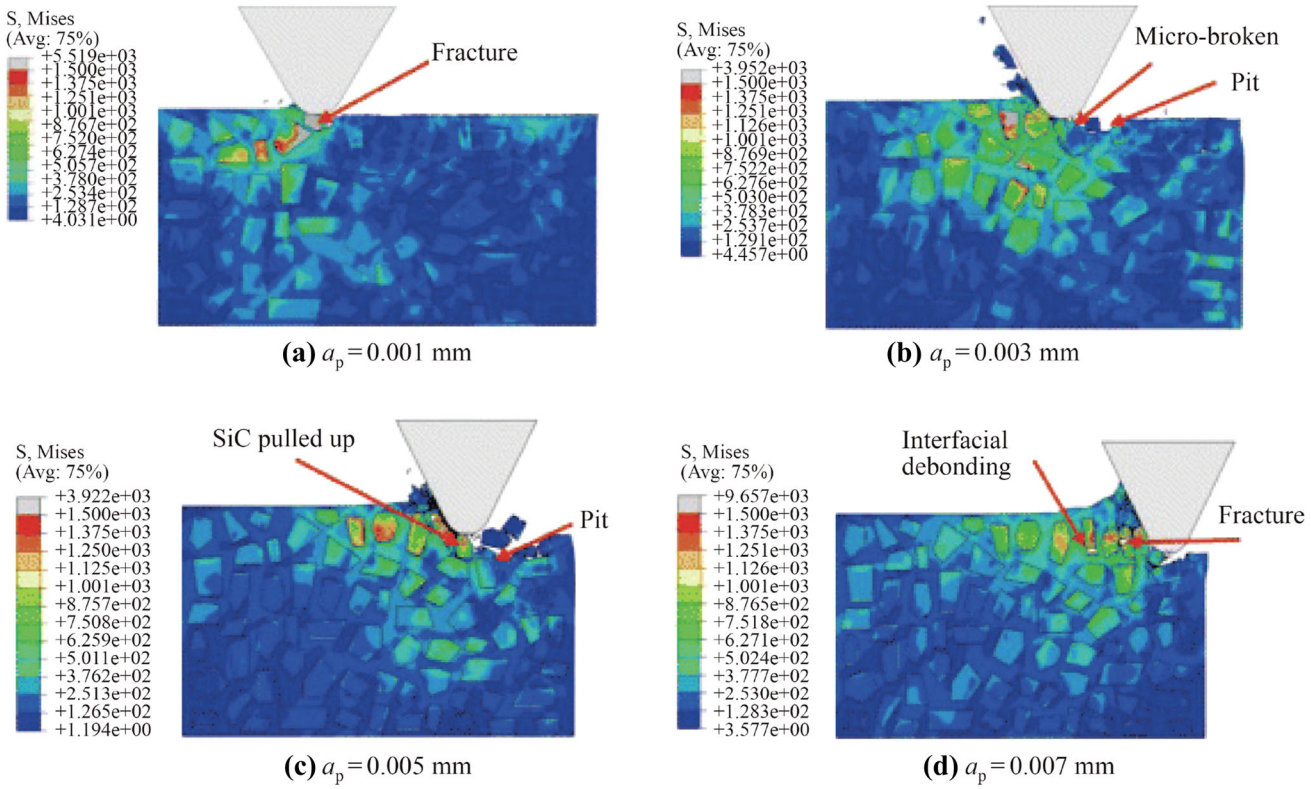

Fig. 19 Machining surface simulation of SiC_p/Al composites at different depths of cut [197]

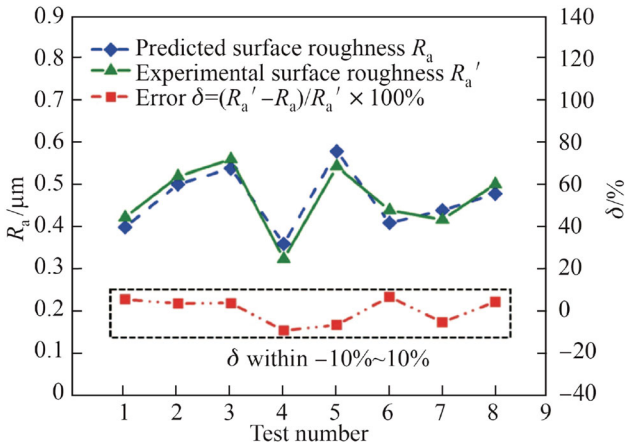

Fig. 20 Predicted and experimental surface roughness [200]

velocity and grinding depth, more serious accumulation and adhesion are found [198]. Among many factors, a clear positive influence of the volume content of the hard phase on the surface finish is observed. Qualitative surface damage through particle fracture pullout appears to be common on most of the finish machined surfaces [199]. Zhu et al. [200] established a theoretical SR model of SiC_p/Al composite grinding based on a combination of the theoretical SR model of aluminum alloy and SiC, as shown in Fig. 20. The exponential composition function proved to be the most suitable, and the coefficients of the function were fitted by the experimental SR.

Pai et al. [201] claimed that the SR improved with an increase in SiC volume percentage and a decrease in depth of cut. This is because an increase in the volume percentage of SiC will increase the hardness of the specimen, which decreases ploughing of the wheel during grinding of a 35% (volume percentage) SiC/Al matrix composite. Hung et al. [202] insisted that a coarse-grit diamond wheel was appropriate for rough grinding, whereas a fine-grit diamond wheel was suitable for fine grinding to achieve the best MMC surface integrity. Nandakumar et al. [203] obtained the best performance by using cashew nut shell oil and nano TiO_2-based minimum quantity lubrication (MQL), because the lubricant of an MQL system penetrated the workpiece and the wheel interface contact zone. Rough grinding with a SiC wheel followed by fine grinding with a fine-grit diamond wheel is recommended for SiC/Al MMCs [189].

3.4.2 Mill grinding, cylindrical grinding, and ductile-regime grinding

The mill grinding uses a grinding head (sintering or plating) that replaces the milling tool to remove the workpiece material with computer numerical control (CNC) milling

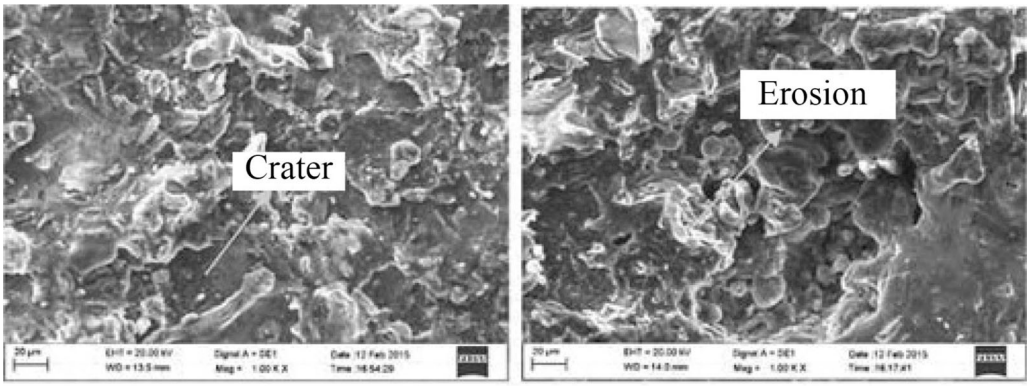

Fig. 21 EDM of SiC/Al MMC **a** crater formation and **b** erosion and pitting on the machined surface [222]

machines. This process has integrated the characteristics embodied in a similar machining route/path as milling and multi-edge continuous cutting as grinding. The cut depth of mill grinding is generally larger to achieve a higher MRR [204]. There are four typical chip shapes, i.e., curved chip, huddled chip, schistose chip, and strip chip, among which, the curved and schistose chips are dominant. The chips generated in mill grinding of SiC_p/Al composites are irregular and uneven under the same machining conditions. During the chip forming, SiC particles can greatly inhibit the deformation of aluminum matrix, and the different contact positions between the SiC particles and diamond grit cause the SiC particles to be fractured, pulled out, and/or pulled into the surface of the chip [205]. The particle fracture and debonding force component in the mill grinding of SiC_p/Al composites can be considered by developing a new force prediction model [206]. Yao et al. [207] recommended a resin-based diamond grinding wheel for 45% (volume fraction) SiC_p/Al composites to achieve the best SR, whereas Li et al. [208] suggested HSS with a super-hard abrasive layer (diamond abrasive and binding agent) to increase the MRR. It is believed that appropriately increasing the feed rate and decreasing the mill-grinding depth can obtain less SR [209]. Based on optimizations, the following parameters are recommended: for SiC/LM25Al (4% (volume fraction)) composites, wheel velocity of 43.9 m/s and workpiece velocity of 26.7 m/min with a feed of 0.056 m/min and depth of cut of 9.1 μm [210]; for 45%(volume fraction) SiC_p/Al composites, wheel speed of 11.77 m/s, feed rate of 100 mm/min, and depth of cut of 0.8 mm [211].

Regarding cylindrical grinding, Thiagarajan et al. [212] suggested cylindrical grinding of 4% (volume fraction) SiC_p/Al using a 60 grit Al_2O_3 wheel at a cutting velocity of grinding wheel of 2639 m/min, cutting velocity of workpiece of 26.72 m/min, feed rate of 0.06 m/min, and depth of cut of 10 μm. The approach for the cylindrical grinding of Al/SiC composites can be extended with super-abrasive grinding wheels such as diamond and CBN.

For ductile-regime grinding, Huang et al. [213] revealed that the critical grinding depth of ductile-regime machining of SiC_p/Al composites decreased with increasing volume fraction of SiC particles due to the decrease in the supporting function of the Al alloy matrix.

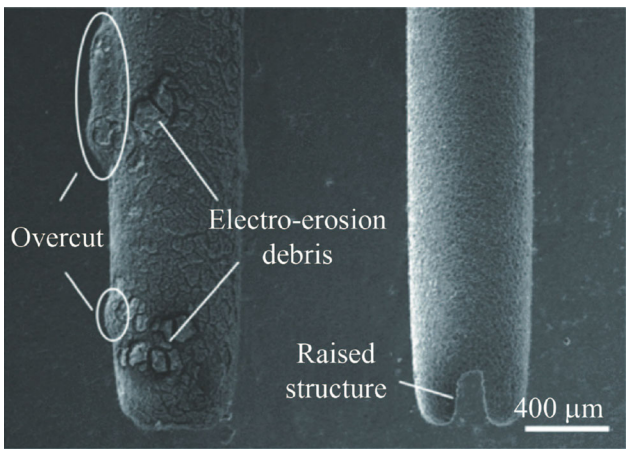

Fig. 22 SEM image of the hole section processed using (left) a cylinder electrode and (right) a tube electrode [224]

4 Nonconventional machining of SiC_p/Al matrix composites

4.1 EDM

EDM is a common nonconventional machining method, which has been widely used in the aerospace, mold, and automobile industries. During machining, a discharge channel is created, where the temperature reaches approximately 12 000 °C, removing material by evaporation and melting from both the electrode and workpiece

Table 4 Recommended parameters for the EDM of SiC_p/Al composites

Tool	Matrix	Fraction	Parameter	Remark
Electrolytic copper electrode of 10 mm diameter [236]	Al 7075	0.5% SiC (mass fraction)	Voltage 47.34 V, pulse current 6 A, pulse on time 8 μs, Pulse on time 9.79 μs	MRR 1.196 g/min TWR 0.001 575 g/min R_a 10.648 μm
Bundled electrode (ϕ 1.2 mm) [237]	Al 6061	5% SiC(volume fraction)	Current 13 A, pulse on time 700 μs, pulse on time 50 μs, flushing pressure 0.040 MPa	Die-sinking EDM
Brass electrode of ϕ 2.7 mm [238]	Components (Al-92.7%, Si-7.0%, Mg-0.3%)	10% SiC (volume fraction)	Current 15 A, pulse on time 1 ms, flushing pressure 0.014 MPa	Maximizing MRR and for minimizing TWR
Copper rod with an array of 2 mm holes (multi-hole) [239]	6061 Al	15% SiC (volume fraction)	Electrode polarity negative, current 4 A, pulse on time 400 μs, pulse on time 10 μs, dielectic pressure 0.05 MPa	Die sinking EDM TWR was 9 mg/min and R_a was 4.78 μm
Brass tool of 15 mm diameter and 60 mm length [240]	Fabricated by stir-casting process	20% SiC	Current 5 A, pulse on time 100 μs, Duty cycle 70%, gap voltage 40 V	Die sinking EDM with positive polarity for electrode
ϕ 12 mm copper and brass cylindrical electrodes [241]	LM_{25}	25% (volume fraction)	Negative current 7.34 A, pulse duration 112 μs, positive: current 6.12 A, pulse duration 108 μs	Copper electrode, maximize MRR with minimum TWR, SR with brass is higher than with copper

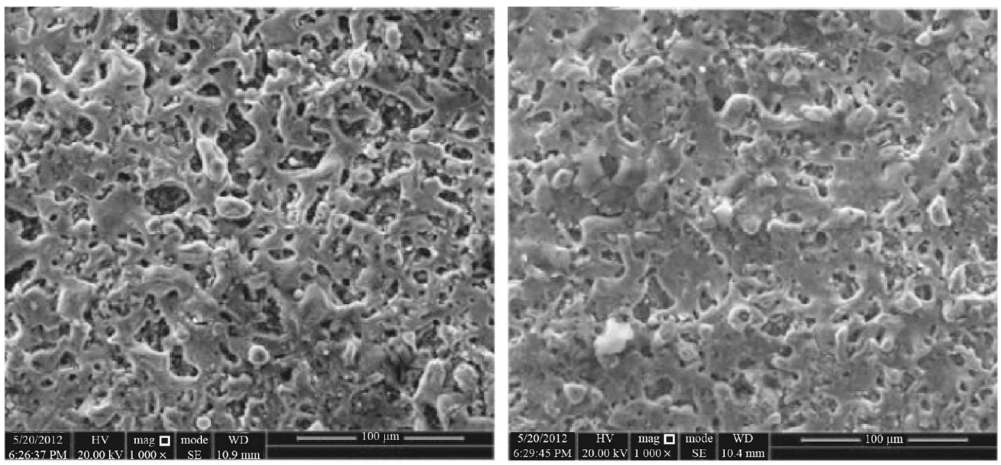

Fig. 23 Environmental SEM microsurface textures **a** after EDM and **b** after PMEDM (40% (volume fraction) SiC/Al-Al powder) [246]

[214]. The MRR and SR are regarded as two indicators of the EDM process, which can evaluate the time of completing the material volume removal and the quality of finished surface, respectively [215]. Additionally, the tool wear ratio (TWR) is also very important for EDM.

The percentage and size of the SiC in SiC/Al MMCs generally have a negative influence on machinability. Karthikeyan et al. [216] revealed that an increase in the volume fraction of SiC decreased the MRR and increased the TWR as well as SR when performing EDM of 6%–20% (volume fraction) SiC/Al composites. Dev et al. [217] reported that an increase in weight percentage of SiC, as well as particle size, had resulted in a decrease in MRR and an increase in TWR and SR. Besides the SiC particles, electrical parameters are the key factors that affect MRR, TWR, and SR. Singh et al. [218] machined an A6061/10% SiC composite and found that with an increase in pulse on time, the MRR, TWR, and SR increase, and the SR increases with an increase in gap voltage. Seo et al. [219] conducted experiments on 15%–35%(volume fraction) SiC_p/Al composites and revealed that the MRR increased with increasing product of peak current and pulse on time

up to an optimal value and then decreased drastically; the combination of low pulse on time and high peak current led to a larger tool wear, higher energy, and rougher surface. It was found that a high current resulted in higher thermal loading on both electrodes (tool and workpiece) leading to a higher amount of material being removed from either electrodes [220]. Surface integrity effects of EDM include roughening of the surface by deposition of a recast layer and pitting of the surface by spark penetration and particulate pullout, as well as surface microcracks [221].

As can be observed from Fig. 21, craters and erosion are evident; metal loss, erosion, and crater formation depend on the intensity of the spark. The high energy of the arc consumed during machining will increase the crater diameter, surface irregularity, and heat-affected zone (HAZ), and the surface will have more ridges and grooves. When adopting a rotating tube electrode, an increase in the rotational speed of the tube electrode can produce a higher MRR and better SR [223]. For instance, Yu et al. [224] machined microholes on a SiC/2024Al workpiece with a cylinder electrode and tube electrode under the same machining conditions. The MRR of EDM with the tube electrode was significantly greater than that of the cylinder electrode. Moreover, the accuracy of EDM holes can be improved by using a tube electrode (rotating speed 800 r/min), as shown in Fig. 22. However, the TWR of a rotating tube electrode tends to be higher and can even be increased by 11.79% compared to that of a cylinder electrode [225]. Regarding the flushing adopted in the EDM of Al/SiC composites, a higher flushing pressure hinders the formation of ionized bridges across the gap and results in a higher ignition delay and decreased discharge energy, thereby decreasing the MRR; however, the SR was found to reduce with an increase in flushing pressure under a certain range [223]. Singh et al. [226] showed that more than 40% reduction in TWR and more than 28% increase in MRR could be achieved by adopting compressed air for the EDM of Al/15% SiC_p ceramic composite.

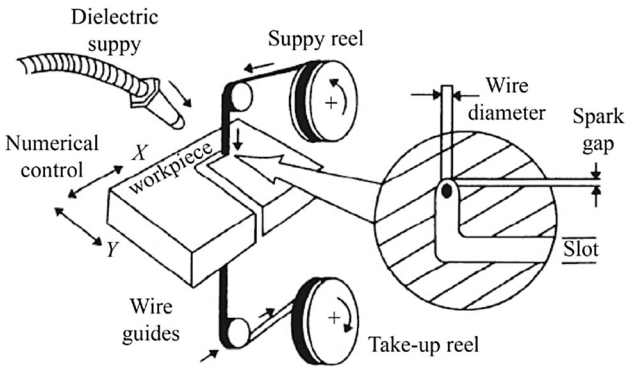

Fig. 24 Schematic of the WEDM process [259, 260]

Attempts for obtaining better parameters to achieve a higher MRR, lower TWR, and better surface quality have been made by many researchers. The optimization of the EDM of Al/SiC composites can be performed by ANNs [227], adaptive neuro-fuzzy inference system [228], fuzzy logic [229], non-dominated sorting genetic algorithm [230], principal component analysis (PCA)—technique for order preference by similarity to ideal solution [231], PCA—fuzzy inference coupled with Taguchi's method [232], and RSM [233–235]. Based on optimizations, the recommended parameters are listed in Table 4 [236–241].

4.2 Powder mixed EDM (PMEDM)

PMEDM is a process variant of EDM, which is performed by adding powder into a dielectric fluid [242]. It has a different machining mechanism from conventional EDM processes. It can improve the SR and is now applied in the finishing stage [243]. The powder particles in the dielectric fluid increase the gap between the tool and the workpiece

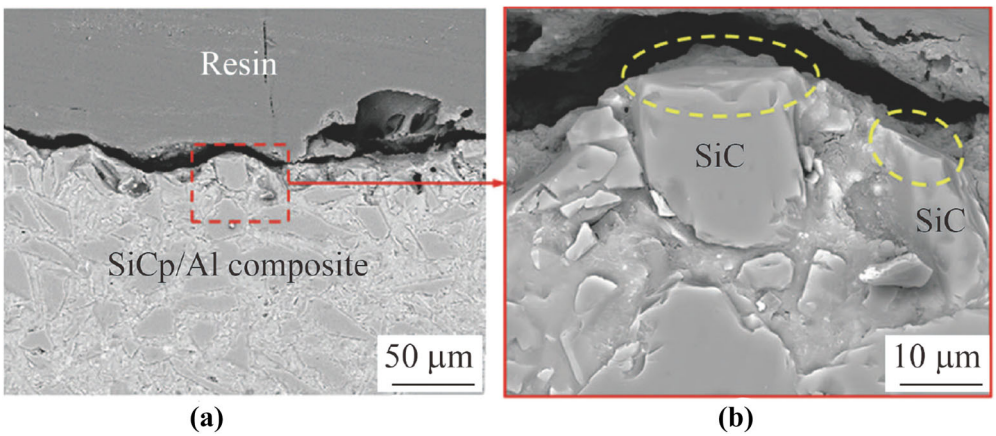

Fig. 25 Microstructure of the residual SiC particles on the surface after the WEDM process **a** SEM observation and **b** magnification of the red box area in **a** [265]

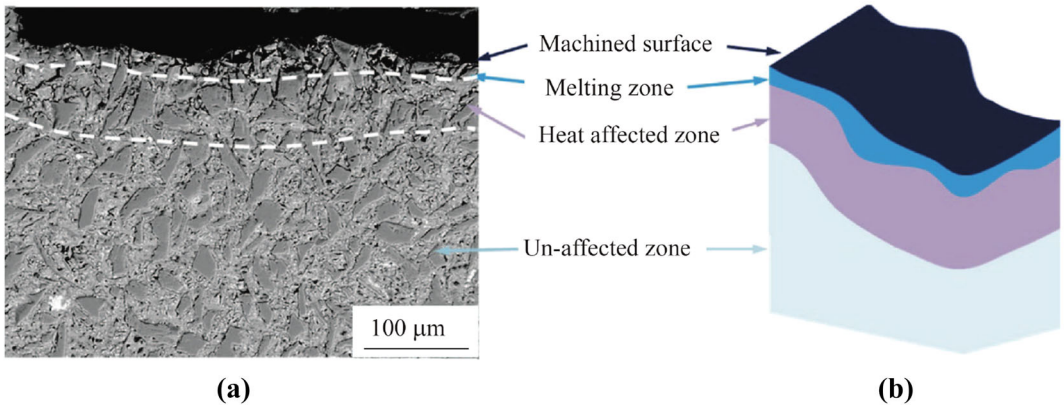

Fig. 26 Cross-sectional microstructure of 65% (volume fraction) SiC_p/2024Al composite after the WEDM process **a** SEM observation result and **b** corresponding schematic [265]

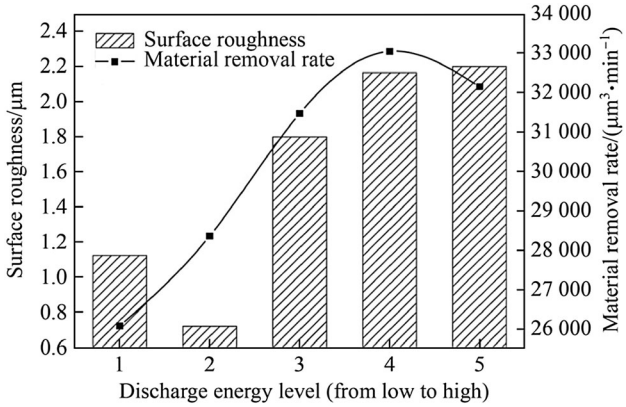

Fig. 27 Effect of discharge energy on surface roughness and material removal rate [268]

while providing a bridging effect between the electrodes for an even distribution of spark energy, making the process more stable [244]. Kansal [245] declared that there was a discernible improvement in the SR of work surfaces after suspending the aluminum powder when machining 10% (volume fraction) SiC_p/Al composites. Hu et al. [246] compared the microsurfaces machined by using EDM and PMEDM, as shown in Fig. 23, and the SR of PMEDM decreased by approximately 31.5%.

Compared to conventional EDM, the presence of tungsten powder in PMEDM resulted in a 48.43% enhancement of MRR in the machining of AA6061/10%SiC composite [247] and 42.85% reduction in the recast layer of the machined surface [248]. The thickness of white recast layer also reduced, whereas the surface hardness was increased with tungsten PMEDM [249]. Besides tungsten powder, carbon nanotubes (CNTs) [250] and multi-walled CNTs [251] are also added in the dielectric to obtain excellent performances in PMEDM of Al/SiC MMCs. Vishwakarma et al. [252] revealed that the PMEDM process provided a better MRR at higher values of peak current, lower concentration of powder, mid-value of gap control, and lower value of duty cycle [253]. Optimization of machining of SiC_p/Al MMCs with PMEDM can be achieved by using the RSM [254], Taguchi and gray analysis [255], ANOVA [256], etc. Kumar and Davim [257] suggested an optimum set of parameters to obtain the highest MRR: powder concentration 4 g/L, pulse duration 100 μs, peak current 9 A, and supply voltage 50 V; for the lowest SR: powder concentration 4 g/L, pulse duration 100 ms, peak current 3 A, and supply voltage 50 V.

4.3 Wire EDM (WEDM)

WEDM differs from conventional EDM, as the electrodes are in the form of a thin wire with a diameter of 0.05–0.3 mm [258]. WEDM is also known as wire electric discharge cutting. The schematic of the WEDM process is presented in Fig. 24 [259, 260].

The electrical conductivity and thermal conductivity of MMCs are lower than those of unreinforced matrix alloys, which decrease the MRR of WEDM [261]. With an increase in the percentage of SiC particles, the machinability of WEDM decreases [262]. An increase of 10% in ceramic reinforcements may lead to an almost 12% reduction in machining efficiency [263]. However, SiC_p/Al composites with high-SiC fractions can still be machined using WEDM [260, 262, 264]. Yang et al. [265] reported the WEDM of a 65% (volume fraction) SiC/2024Al composite and proposed that the machining mechanism was a combination of melting of the Al matrix and decomposition of SiC particles. Figure 25 illustrates the microstructure of the residual SiC particles on the surface after the WEDM process. Figure 26 shows a cross-sectional microstructure of the WEDM of the 65% (volume fraction) SiC/2024Al.

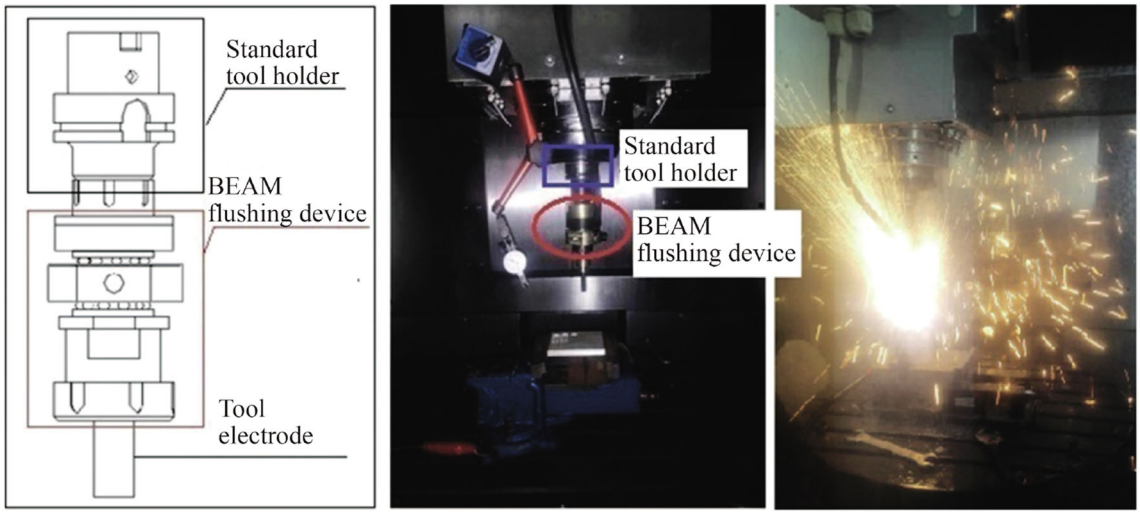

Fig. 28 BEAM flushing device and arc discharge schematic [281]

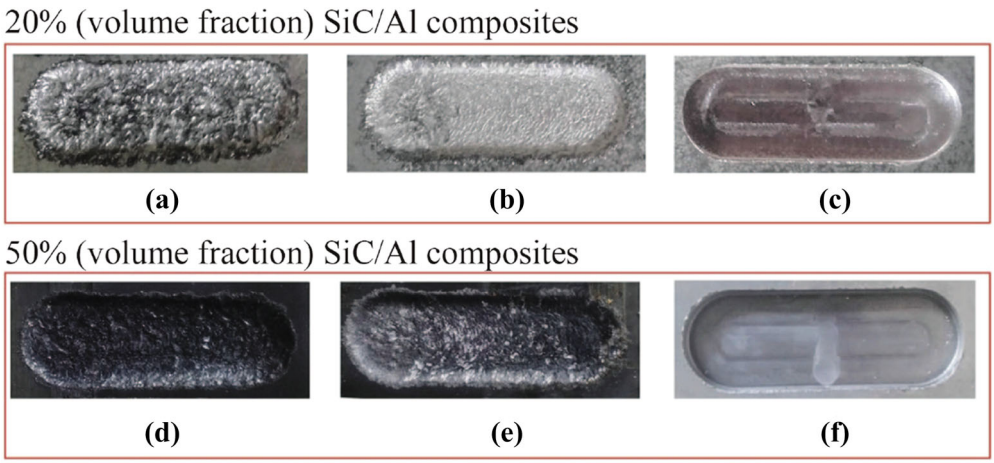

Fig. 29 Machined surface comparison **a** negative BEAM-20% (volume fraction) SiC/Al, **b** positive BEAM-20% (volume fraction) SiC/Al, **c** milling-20% (volume fraction) SiC/Al, **d** negative BEAM-50% (volume fraction) SiC/Al, **e** positive BEAM-50% (volume fraction) SiC/Al, **f** milling-50% (volume fraction) SiC/Al [281]

Pramanik [266] observed a significant variation in the wire diameter during machining of SiC particles reinforced with 6061 aluminum alloy. The variation was mainly caused by the presence or absence of the matrix material coating on the wire, which might cause uncontrolled spark and variation in the ability of electrolytes. Wire breakage is a limitation on the MRR, which can be observed when machining Al/SiC composites. However, wire breakages can be reduced by employing higher flushing pressures, higher pulse off times, and suitable values of servo reference voltage. In general, it was suggested that large pulse on time, high flushing pressure, appropriate wire speed and wire tension, large pulse off time, and appropriate pulse current should be used to obtain optimum machining performance [267]. Figure 27 displays the effect of discharge energy on SR and MRR during the WEDM of 45% (volume fraction) SiC_p/Al [268]. It can be observed that the discharge energy presents a strong relationship with machinability by affecting the SiC thermal status.

Different from the conventional WEDM, the dry WEDM was adopted as an environmentally friendly modification of the oil WEDM process, in which the liquid dielectric is replaced by a gaseous medium. An Al 6061C 25% SiC workpiece has been machined with dry WEDM by Fard et al. [228]. Moreover, WEDM was modified to machine a SiC/Al7075 MMC using a wire electrical discharge turning (WEDT) process. WEDT was found to have advantages over the conventional turning process [269]. Many optimizations have been conducted to predict the machining performance or improve the machinability of

SiC/Al MMCs, e.g., ANN-RSM [270], RSM [271–274], Taguchi's approach [275], Taguchi-based hybrid gray-fuzzy grade approach [276], particle swarm optimization [277], AHP-TOPSIS (a hybrid approach obtained by integrating the AHP with TOPSIS technique) [278], and non-dominated sorting genetic algorithm [279].

4.4 ADM

To some extent, ADM is similar to EDM, but ADM adopts arc discharge whereas EDM utilizes spark discharge. Generally, the machining efficiency of ADM is much higher than that of EDM. Blasting erosion arc machining (BEAM) was one type of ADM, which was developed recently by Zhao et al. [11]. BEAM has been adopted in the processing of SiC_p/Al composites to improve the machining efficiency [280]. A flushing system is necessary to conduct BEAM. Figure 28 depicts a flushing device that can be fixed on a standard tool holder [281].

Gu et al. [282] machined a 20% (volume fraction) SiC_p/Al composite and achieved a high MRR of 8276 mm^3/min (peak current of 500 A) with a specific MRR of 16.4 mm^3/(A·min). Compared to the EDM MRR of 140 mm^3/min (peak current of 100 A) with a specific MRR 1.4 mm^3/(A·min) [219], the efficiency of BEAM is much higher. Chen et al. [283] also conducted experiments on the machining of 50% (volume fraction) SiC_p/Al. The results revealed that even for the high-SiC fraction SiC_p/Al composites, BEAM still could be used and the obtained MRR was as high as 7 500 mm^3/min. It was reported that BEAM could also be used for other difficult-to-machine materials, such as titanium alloys [284] and nickel-based superalloys [285]. As shown in Fig. 29, both positive and negative polarity machining can be adopted in BEAM; however, the machined surface qualities are generally not the same. Generally, positive BEAM tends to obtain a better surface but a lower efficiency and higher TWR. The side effect of BEAM is a rough surface, but fortunately, this problem can be solved by adopting combined machining of CNC, as reported by Chen et al. [281].

4.5 ECM

ECM is based on a controlled anodic electrochemical dissolution process of the workpiece with the tool as the cathode in an electrolytic cell [286].

By analyzing the influence of the current density in the ECM of 10% SiC/Al MMC, it was found that feed velocity could be approached by a linear function beginning in the origin of ordinates, which led to an active dissolution of the workpiece material, at a low current density of 4 A/cm^2, an SR of 0.65 μm was achieved. The roughness was decreased to 0.2 μm at 10 A/cm^2 [287]. Kumar and Sivasubramanian [288] compared the ECM of an A356 aluminum alloy reinforced with 5%, 10%, and 15% (mass fraction) SiC particles. They found that the maximum MRR was obtained by applying the least voltage and least SiC content, a moderate value of electrode feed rate, and the highest electrolyte concentration. Senthilkumar et al. [289] illustrated that an increase in the applied voltage, flow rate, and electrolyte concentration resulted in a higher MRR. The optimized parameters for the ECM of LM25 Al/10% SiC were as follows: electrolyte concentration 12.53 g/L, electrolyte flow 7.51 L/min, applied voltage 13.5 V, feed rate 1 mm/min. The corresponding MRR was 0.877 3 g/min and the SR was 6.566 7 μm. An optimal machining parametric combination for the ECM of LM25-25% (volume fraction) SiC, i.e., electrolyte concentration 22.74 g/L, electrolyte flow rate 7.57 L/min, applied voltage 14.8 V, and tool feed rate 0.902 mm/min, was found out to achieve a maximum MRR of 0.051 3 g/min and minimum R_a of 7.013 8 μm [290]. Another group of optimal parameters for the ECM of 10%(mass fraction) SiC/Al matrix composites was obtained by Dharmalingam et al. [291]. The optimal values for maximum MRR were machining voltage 7 V, electrolyte concentration 24 g/L, and frequency 50 Hz. The optimal values for minimum overcut were machining voltage 9 V, electrolyte concentration 18 g/L, and frequency 50 Hz. Lehnert et al. [292] adopted an electrochemical precision machining process for complex geometries. A voltage of 16 V and a feed rate of 0.25 mm/min to generate the geometry with the smallest extent were suggested.

4.6 Abrasive waterjet (AWJ) cutting

AWJ machining has many advantages compared to other machining technologies. In contrast to thermal machining processes (laser and EDM), AWJ does not induce high temperatures, and thus, there is no HAZ [293]. In the AWJ machining process, the workpiece material is removed by the action of a high-velocity jet of water mixed with abrasive particles based on the principle of erosion of the material upon which the waterjet hits [294, 295]. It is believed that the AWJ machining can be a real competitor of the current techniques employed for cutting super-abrasive materials [296]. Early in the 1990s, AWJ had been used for the cutting of a 30%(volume fraction) SiC particulate/6061 matrix composite plate with a thickness of 5.08 mm. The MMC plate was easily machined and good surface finish was produced [297]. Srinivas and Babu [298] observed the cut surfaces with SEM, as shown in Fig. 30, and proposed a possible mechanism of material removal, which was the fracturing and ploughing of SiC and the ductile fracturing of the matrix material.

Based on experiments performed on SiC/Al matrix composites with different SiC mass fractions (5%–20%), Srinivas and Babu [299] suggested that appropriate choices of abrasive mass flow rates and jet traverse speeds were of considerable importance over other parameters such as waterjet pressure. Patel and Srinivas [300] employed an AWJ to perform similar turning of an aluminum-SiC MMC and showed that AWJ could be suitable for turning MMCs without the problems encountered in conventional turning such as tool wear. In addition, it was found that the traverse rate and nozzle angle influence the SR and MRR more than the SiC contents.

4.7 Laser machining (cutting)

Laser machining offers significant advantages for rough cut-off applications. Laser is very suitable for machining at high feed rates (up to 3 000 mm/min) and can produce a cut with a narrow kerf width (0.4 mm). However, the quality of the laser-cut surface is relatively poor, e.g., striation patterns on the cut surface, burrs at the exit of the laser, and significant thermally induced microstructural changes can be observed [293]. Sharma and Kumar [301] reported that the most prominent input parameters of laser cutting of AA5052/SiC were cutting speed, reinforced SiC particles, and arc radius. The formations of a recast layer and new phase Al_4C_3 were detected respectively. When the reinforced SiC particle quantity was fixed at 20% (mass fraction) and the nozzle standoff distance was decreased from 2 mm to 1 mm, the dross height increased from 0.373 mm to 0.481 mm [302]. Figure 31 displays a group of SEM images of surfaces cut by a laser beam process. Unburned SiC particles (marked in circular dashed line) and restricted flow of molten material into a downward direction can be observed.

The laser beam can also be utilized as a cutter or driller to conduct turning or drilling. For example, Biffi et al. [303] used a short-duration laser beam as a tool and cut a thread in an A359-20% SiC composite material (although with limited removal rates). Padhee et al. [304] employed a laser beam and drilled holes on 15% (mass fraction)SiC/Al matrix composites (limited to microhole drilling).

4.8 Jet-ECM

Jet-ECM is a technology for quickly and flexibly generating microstructures and microgeometries in metallic parts regardless of the material hardness and without any thermal or mechanical impact [305, 306]. As indicated in Fig. 32, the electrolytic liquid is pumped through a small nozzle and ejected with a mean velocity of approximately 20 m/s to form a free jet [307]. By using a pulsation-free pump, a continuous supply of fresh electrolyte with constant pressure is assured to generate a well-defined geometrical shape [305].

The dissolution characteristic in the machining of SiC/Al MMCs utilizing Jet-ECM varies with the electrolyte used. When using $NaNO_3$, the depth and width were hardly affected by the particle fraction, however, in the case of NaCl and NaBr, the particles significantly influenced both the width and depth [308]. Figure 33 shows that the aqueous electrolytes of $NaNO_3$ and NaCl produce different electrochemical dissolution characteristics [309]. While the diameters of the calottes created with both electrolytes are similar, the use of NaCl electrolyte results in significantly deeper calottes for machining times of approximately 1.5–2 s.

5 Conventional and nonconventional hybrid machining of SiC_p/Al matrix composites

5.1 Laser-assisted machining (LAM)

Compared with the conventional cutting process, LAM [310–314] heats the workpiece with a laser beam to change the microstructure or locally harden the material near the cutting tool. To date, most investigations regarding LAM

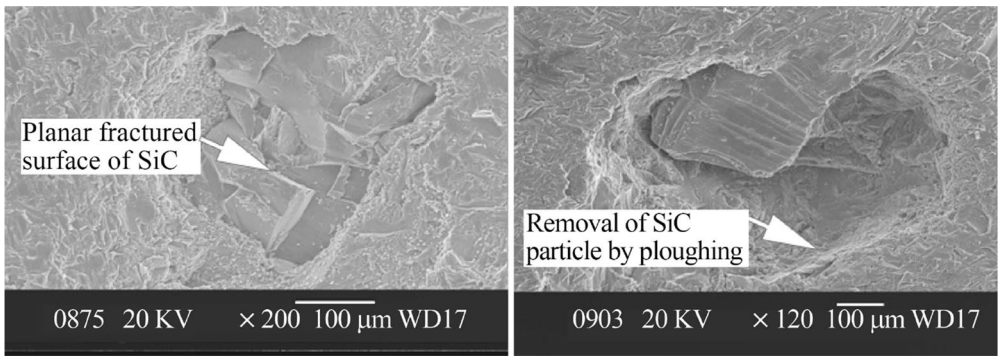

Fig. 30 SEM photograph showing cutting of SiC reinforcement by 60 mesh size garnet abrasives in AWJ (10%SiC_p-MMC) [298]

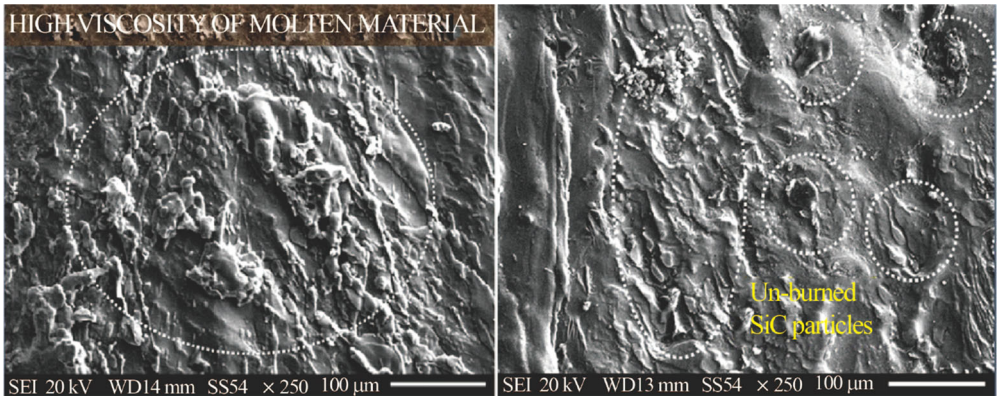

Fig. 31 SEM micrograph showing unburned SiC reinforced particles and restricted flow (20% SiC/Al) [301]

of SiC_p/Al matrix composites are focused on laser-assisted turning.

Figure 34 presents a schematic of the laser-assisted turning. The LAM process demonstrates a considerable improvement in the machining of MMCs through a lower tool wear and thus increased tool life, as well as reduction in cutting time [315].

LAM provides a higher MRR under the same SR compared to conventional machining. LAM reduced the machining time of Al/SiC_p/45% MMCs by 45% due to fewer tool changes, high MRR, and longer tool life compared to conventional machining, the shorter machining time and longer tool life provide a 40%–50% cost saving per part, but with the additional cost of a graphite coating and diode laser [316]. Figure 35 illustrates a comparison of tool (uncoated and coated) life for conventional machining and LAM.

Kawalec et al. [317] found a decrease in cutting force during LAM of aluminum matrix composites compared to conventional turning. Kong et al. [318] explained that abrasive tool wear was the most dominant wear mechanism for three different WC tools in the LAM of SiC_p/45% composites. The adhesion wear and diffusion wear were accelerated to some extent with increasing temperature.

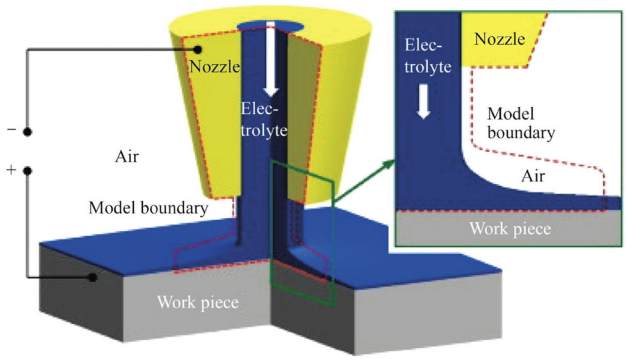

Fig. 32 Principle of Jet-ECM [307]

5.2 Ultrasonic assisted machining (UAM)

UAM or ultrasonic vibration machining is a hybrid process. It can reduce the influence of tearing, plastic deformation, and BUE in cutting and can restrain flutter, making the cutting process more stable [319]. By employing an ultrasonic-vibration source, conventional cutting processes can be modified as ultrasonic vibration–assisted processes. Typical UAM processes are ultrasonic assisted turning [320, 321], ultrasonic assisted milling [322, 323], ultrasonic assisted drilling [324, 325], and ultrasonic assisted grinding [326–328].

Ultrasonic assisted turning shows improvement in both cutting force and surface topography compared to conventional turning [321]. Zhong and Lin [320] reported that the roughness of an MMC A359/SiC/20p surface turned with vibration was better than that turned without vibrations. In ultrasonic milling, the SiC particle removal form can be classified into type of cut, pulled, pressed, and crack penetration; increasing the number of SiC particle cut type results in better surface smoothness [323]. Xiang et al. [322] reported that a superior roughness of ultrasonic assisted milling of 65% (volume fraction) SiC/Al composites could be obtained at a cutting speed 160 m/min, feed rate 0.02 mm/z, and depth of cut 0.2 mm. During the ultrasonic vibration drilling, the SiC particle in the composites tended to break along the crystal connection boundary or suffer ductile fracture under the dynamic ultrasonic impulse, in which the cutting resistance could be reduced and the tool edge could be protected. Thereby, the drilling location precision and hole surface quality were enhanced; the wear of the drill chisel edge was effectively improved, and the drilling torque was reduced by approximately 30% [324]. Ultrasonic vibration produces a smaller burr height and width in the drilling of Al/SiC MMC. The burr height and width in UAM are respectively 83% and 24% lower than those in conventional drilling [325]. In ultrasonic grinding, the grinding force and SR were found

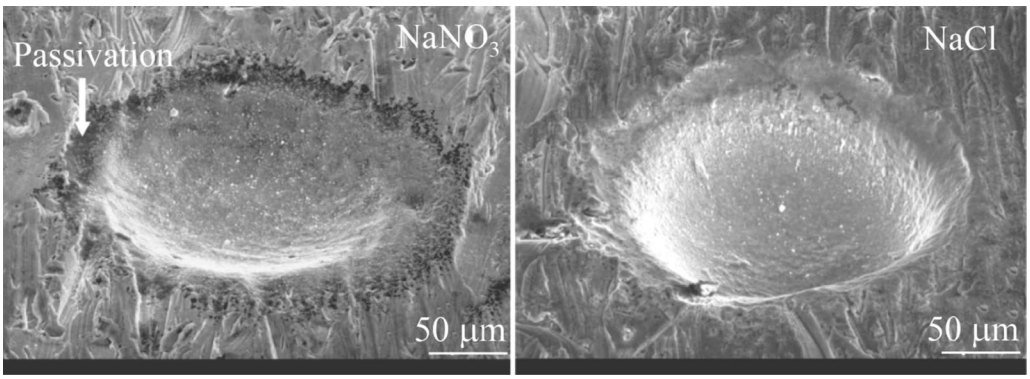

Fig. 33 Images of calottes on EN AW 2017 + 10% SiC particles machined with aqueous electrolytes of $NaNO_3$ and NaCl [309]

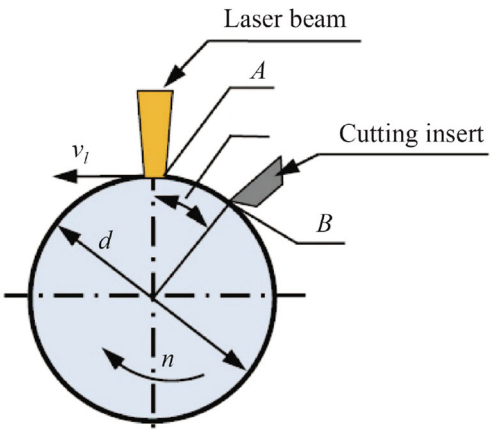

Fig. 34 Schematic of the laser-assisted machining process (*A* heating area of the laser beam; *B* zone of machining; *d* workpiece diameter) [315]

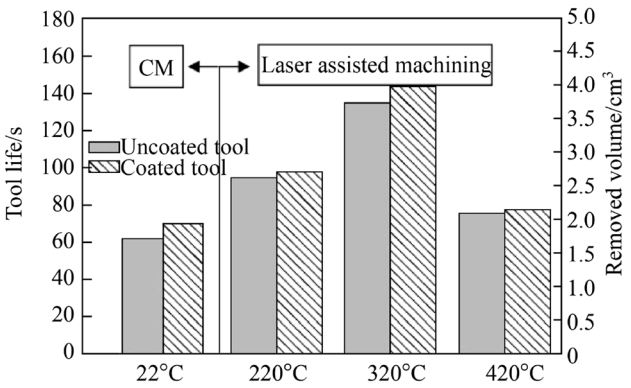

Fig. 35 Tool life of uncoated and coated tools in conventional machining (CM) and laser-assisted machining [316]

lower than those in ordinary grinding for the same grinding parameters [326, 327]. The reduction in cutting force and SR can reach 13.86% and 11.53%, respectively [329]. Zheng et al. [328] showed some optimum conditions for the grinding of 45% SiC_p/Al2024 composites using ultrasonic vibration. For a minimum value of SR, the parameters were as follows: spindle speed 15 000 r/min, vibration amplitude 5 μm, cutting depth 15 μm, and feed rate 5 mm/min.

5.3 Other hybrid machining technologies

The electrolytic in-process dressing (ELID) technique applies an electric current during the conventional grinding process. Shanawaz et al. [330] employed ELID for the machining of low fraction SiC_p/Al composites and found that a smoother surface could be obtained at a high current duty ratio. Yu et al. [331] obtained a high-integrity machined surface for a high-SiC fraction (56%(volume fraction)) SiC_p/Al composite. On the workpiece surface, most of the SiC particles were removed in ductile mode, and the brittle fracture of SiC particles was reduced substantially.

Surface-electrical discharge diamond grinding consists of diamond grinding and EDM with a rotating disk, which can enhance the MRR and produce a better surface finish [332]. Agrawal and Yadava [333] found the best combination of processing 10% (mass fraction)Al/SiC, which was as follows: wheel speed 1 400 r/min, table speed 4 mm/s, in feed 20 m, current 24 A, pulse on time 50 μs, and duty factor 0.817.

The waterjet-guided (WJG) laser process uses a pressurized microwaterjet as a laser beam guide. Marimuthu et al. [334] conducted an experiment on the WJG laser drilling of 40% (volume fraction) SiC reinforced aluminum MMCs. The advantages found include high levels of hole circularity, no HAZ, no recast layer, and no changes in microstructure.

Electrochemical discharge machining (ECDM) combines the actions of EDM and ECM. Liu et al. [335] employed ECDM to machine 20% (volume fraction) SiC/Al matrix composites and revealed that smaller median and maximal debris sizes were found in the ECDM process, which indicated that the arc energy of ECDM was likely to

be smaller than that of the EDM process (which could be explained from the aspect of total energy).

6 Conclusions

This review has summarized the aspects regarding the machinability of SiC_p/Al composites with conventional machining, i.e., turning, milling, drilling, and grinding, and nonconventional machining, i.e., EDM, PMEDM, WEDM, ECM, AWJ, Jet-ECM, and newly developed high-efficiency machining technologies. Machining efficiency, surface quality, and tool wear need to be first considered regardless of the machining method. With conventional machining methods, the machining efficiency tends to be enhanced by increasing machining parameters such as machining speed, cutting depth, and feed rate; however, the increased parameters can easily intensify tool wear and shorten tool life. Besides, different SiC fractions of SiC_p/Al composites also present different degrees of influence on the machining mechanism, tool wear mechanism, chip formation, and even the machined surface integrity. Higher percentages of SiC particles are more likely to result in a lower machining efficiency and higher tool wear. Hence, various optimization methods, i.e., ANOVA and gray relational analysis, regression models, ANN models, and response surface methodology can be employed to find the most suitable machining condition.

For the nonconventional machining of SiC_p/Al, i.e., EDM, PMEDM, WEDM, ECM, Jet-ECM, and AWJ, it is believed that the SiC particles can interfere with the electrical discharges during the EDM of SiC_p/Al. Hence, the MRR, TWR, and surface quality are strongly related to the electrical parameters, i.e., gap voltage, peak current, pulse on time, and pulse off time. Moreover, non-electrical parameters such as flushing can affect machinability, e.g., a higher flushing pressure can decrease the discharge energy and reduce the MRR. One of the main problems encountered with the nonconventional machining of SiC_p/Al is the relatively low machining efficiency. However, this problem can be partly solved by adopting newly developed high-efficiency arc discharge technologies, e.g., BEAM, where the achieved MRR can be hundreds times higher than that of the conventional EDM. The drawback of the arc discharge is the rough machined surface, but fortunately, this can be eliminated by a combination of conventional cutting processes. Hence, employing of arc discharge to obtain a high MRR and the combination of conventional cutting to achieve a fine surface quality may be an efficient and economical way of machining SiC_p/Al composites.

In recent years, an increasing number of SiC_p/Al composites with high-SiC fraction, e.g., 50%, 55%, and 65% (volume fraction), have attracted the attention of investigators. For these high-SiC fraction SiC_p/Al composites, turning and milling processes are generally adopted, and nonconventional processes such as EDM, BEAM, and Jet-ECM are also preferred by researchers. It is concluded that there will be more machining methods and investigations regarding high-SiC fraction SiC_p/Al composites in the future.

Acknowledgements This work was supported by National Natural Science Foundation of China (Grant Nos. 51975371 and 51575351), Innovation and entrepreneurship project for high-level talents in Jiangsu province (Grant No. 164040022), Youth science and technology innovation fund of NJFU (Grant No. CX2018017), PNFD (a project funded by the National First-class Disciplines), and PAPD (a project funded by the Priority Academic Program Development of Jiangsu Higher Education Institutions).

References

1. Nicholls CJ, Boswell B, Davies IJ et al (2017) Review of machining metal matrix composites. Int J Adv Manuf Technol 90:2429–2441
2. Sidhu SS, Batish A, Kumar S (2013) Fabrication and electrical discharge machining of metal-matrix composites: a review. J Reinf Plast Compos 32(17):1310–1320
3. Benal MM, Shivanand HK (2006) Influence of heat treatment on the coefficient of thermal expansion of Al (6061) based hybrid composites. Mater Sci Eng A 435/436(6):745–749
4. Mishra AK, Srivastava RK (2017) Wear behaviour of Al-6061/SiC metal matrix composites. J Inst Eng 98(2):97–103
5. Reddy AP, Krishna PV, Rao RN (2017) Al/SiC NP and Al/SiC NP/X nanocomposites fabrication and properties: a review. Proc Inst Mech Eng Part N J Nanomater Nanoeng Nanosyst 231(4):155–172
6. Xiang J, Pang S, Xie L et al (2018) Investigation of cutting forces, surface integrity, and tool wear when high-speed milling of high-volume fraction SiCp/Al6063 composites in PCD tooling. Int J Adv Manuf Technol 98(5/8):1237–1251
7. Tailor S, Mohanty R, Soni P et al (2016) Wear behavior of plasma sprayed nanostructured Al-SiC composite coatings: a comparative study. Trans Indian Inst Met 69(6):1179–1191
8. Bushlya V, Lenrick F, Gutnichenko O et al (2017) Performance and wear mechanisms of novel superhard diamond and boron nitride based tools in machining Al-SiC_p metal matrix composite. Wears 376/377:152–164

9. Bains PS, Sidhu SS, Payal H (2016) Fabrication and machining of metal matrix composites: a review. Mater Manuf Process 31(5):553–573
10. Chambers AR (1996) The machinability of light alloy MMCs. Compos A Appl Sci Manuf 27(2):143147
11. Zhao W, Gu L, Xu H et al (2013) A novel high efficiency electrical erosion process-blasting erosion arc machining. Procedia CIRP 6:621–625
12. Ramnath BV, Elanchezhian C, Annamalai R et al (2014) Aluminium metal matrix composites-a review. Rev Adv Mater Sci 38(5):55–60
13. Shukla M, Dhakad S, Agarwal P et al (2018) Characteristic behavior of aluminium metal matrix composites: a review. Mater Today Proc 5(2):5830–5836
14. Soltani S, Khosroshahi RA, Mousavian RT et al (2017) Stir casting process for manufacture of Al-SiC composites. Rare Met 36(7):581–590
15. Kainer K (2006) Custom made materials for automotive and aerospace engineering. Metal matrix nanocomposites. Wiley, Weinheim, pp 1–48
16. Muraliraja R, Arunachalam R, Al-Fori I et al (2019) Development of alumina reinforced aluminum metal matrix composite with enhanced compressive strength through squeeze casting process. Proc Inst Mech Eng Part L J Mat Des Appl 233(3):307–314
17. Sarfraz S, Jahanzaib M, Wasim A et al (2017) Investigating the effects of as-casted and in situ heat-treated squeeze casting of Al-3.5% Cu alloy. Int J Adv Manuf Technol 89(9/12):3547–3561
18. Sarfraz MH, Jahanzaib M, Ahmed W et al (2019) Multi-response parametric optimization of squeeze casting process for fabricating Al 6061-SiC composite. Int J Adv Manuf Technol 102(1/4):759–773
19. Kini UA, Sharma S, Jagannath K et al (2015) Characterization study of aluminium 6061 hybrid composite. Int J Chem Mol Nucl Mater Metall Eng 9(6):578–582
20. Falsafi J, Rosochowska M, Jadhav P et al (2017) Lower cost automotive piston from 2124/SiC/25p metal-matrix composite. SAE Int J Engines 10(4):1984–1992
21. Avci U, Temiz S (2017) A new approach to the production of partially graded and laminated composite material composed of SiC-reinforced 7039 Al alloy plates at different rates. Compos B Eng 131:76–81
22. Lee H, Choi JH, Jo MC et al (2018) Effects of strain rate on compressive properties in bimodal 7075 Al-SiC_p composite. Met Mater Int 24(4):894–903
23. Rodrıguez-Castro R, Wetherhold R, Kelestemur M (2002) Microstructure and mechanical behavior of functionally graded Al A359/SiC_p composite. Mater Sci Eng A 323(1/2):445–456
24. Surappa M, Surappa MK (2008) Dry sliding wear of fly ash particle reinforced A356 Al composites. Wear 265(3/4):349–360
25. Chakraborty S, Kar S, Ghosh SK et al (2017) Parametric optimization of electric discharge coating on aluminium-6351 alloy with green compact silicon carbide and copper tool: a Taguchi coupled utility concept approach. Surf Interfaces 7:47–57
26. Murty SN, Rao BN, Kashyap B (2002) On the hot working characteristics of 2124 Al-SiC_p metal matrix composites. Adv Compos Mater 11(2):105–120
27. Karvanis K, Fasnakis D, Maropoulos A et al (2016) Production and mechanical properties of Al-SiC metal matrix composites. IOP Conf Ser Mater Sci Eng 161:012070
28. Min S (2009) Effects of volume fraction of SiC particles on mechanical properties of SiC/Al composites. Trans Nonferrous Met Soc China 19(6):1400–1404
29. Ozben T, Kilickap E, Cakır O (2008) Investigation of mechanical and machinability properties of SiC particle reinforced Al-MMC. J Mater Process Technol 198(1/3):220–225
30. Milan M, Bowen P (2004) Tensile and fracture toughness properties of SiC reinforced al alloys: effects of particle size, particle volume fraction, and matrix strength. J Mater Eng Perform 13(6):775–783
31. El-Kady O, Fathy A (2014) Effect of SiC particle size on the physical and mechanical properties of extruded Al matrix nanocomposites. Mater Des (1980–2015) 54:348–353
32. Hong SJ, Kim HM, Huh D et al (2003) Effect of clustering on the mechanical properties of SiC particulate-reinforced aluminum alloy 2024 metal matrix composites. Mater Sci Eng, A 347(1/2):198–204
33. Yan C, Lifeng W, Jianyue R (2008) Multi-functional SiC/Al composites for aerospace applications. Chin J Aeronaut 21(6):578–584
34. Huang Y, Chen G, Wang B et al (2019) Fabrication, microstructure and properties of the mid-fraction SiC particles/6061Al composites using an optimized powder metallurgy technique. Russ J Non-Ferrous Met 60(3):312–318
35. Muthukrishnan N, Murugan M, Rao KP (2008) An investigation on the machinability of Al-SiC metal matrix composites using PCD inserts. Int J Adv Manuf Technol 38(5/6):447–454
36. Das S, Behera R, Majumdar G et al (2007) An experimental investigation on the machinability of powder formed silicon carbide particle reinforced aluminium metal matrix composites. Int J Heat Mass Transf 50(25/26):5054–5064
37. Dabade UA, Joshi SS, Balasubramaniam R et al (2007) Surface finish and integrity of machined surfaces on Al/SiC_p composites. J Mater Process Technol 192/193(1):166–174
38. Ciftci I, Turker M, Seker U (2004) CBN cutting tool wear during machining of particulate reinforced mmcs. Wear 257(9/10):1041–1046
39. Ge Y, Xu J, Yang H (2010) Diamond tools wear and their applicability when ultra-precision turning of SiC_p /2009Al matrix composite. Wear 269(11/12):699–708
40. Chou YK, Liu J (2005) CVD diamond tool performance in metal matrix composite machining. Surf Coat Technol 200(56):1872–1878
41. Xiang J, Xie L, Gao F et al (2018) Diamond tools wear in drilling of SiC_p /Al matrix composites containing copper. Ceram Int 44(5):5341–5351
42. Durante S, Rutelli G, Rabezzana F (1997) Aluminum-based MMC machining with diamond-coated cutting tools. Surf Coat Technol 94:632–640
43. Karabulut S, Karako H (2017) Investigation of surface roughness in the milling of Al7075 and open-cell SiC foam composite and optimization of machining parameters. Neural Comput Appl 28(5):313–327
44. Sahin Y (2005) The effects of various multilayer ceramic coatings on the wear of carbide cutting tools when machining metal matrix composites. Surf Coat Technol 199(1):112–117
45. Errico GE, Calzavarini R (2001) Turning of metal matrix composites. J Mater Process Technol 119(13):257–260
46. Andrewes CJE, Feng HY, Lau WM (2000) Machining of an aluminum/SiC composite using diamond inserts. J Mater Process Technol 102(13):25–29
47. Yousefi R, Kouchakzadeh MA, Rahiminasab J et al (2011) The influence of SiC particles on tool wear in machining of Al/SiC metal matrix composites produced by powder extrusion. Adv Mater Res 325:393–399
48. Manna A, Bhattacharayya B (2005) Influence of machining parameters on the machinability of particulate reinforced Al/SiC MMC. Int J Adv Manuf Technol 25(9/10):850–856

49. Hooper RM, Henshall JL, Klopfer A (1999) The wear of polycrystalline diamond tools used in the cutting of metal matrix composites. Int J Refract Metal Hard Mater 17(13):103–109
50. Malli NA, Aaditya V, Raghavan R (2012) Study and analysis of PCD 1500 and 1600 grade inserts on turning Al 6061 alloy with 15% reinforcement of SiC particles on MMC. Int Proc Comput Sci Inf Technol 31:143–148
51. Klkap E, Akr O, Aksoy M et al (2005) Study of tool wear and surface roughness in machining of homogenised SiC reinforced aluminium metal matrix composite. J Mater Process Technol 164/165(10):862–867
52. Kremer A, Devillez A, Dominiak S et al (2008) Machinability of Al/SiC patriculate metal-matrix composites under dry conditions with CVD diamod-coated cabride tools. Mach Sci Technol 12(2):214–233
53. Karthikeyan R, Ganesan G, Nagarazan RS et al (2001) A critical study on machining of Al/SiC composites. Adv Manuf Process 16(1):47–60
54. Manna A, Bhattacharayya B (2003) A study on machinability of Al/SiC-MMC. J Mater Process Technol 140(1/3):711–716
55. Ciftci I (2009) Cutting tool wear mechanism when machining particulate reinforced MMCs. Technology 12(4):275–282
56. Bhushan RK (2013) Multiresponse optimization of Al alloy-SiC composite machining parameters for minimum tool wear and maximum metal removal rate. J Manuf Sci Eng 135(2):021013
57. Das D, Chaubey AK, Nayak BB et al (2018) Investigation on cutting tool wear in turning Al 7075/SiC_p metal matrix composite. IOP Conf Ser Mater Sci Eng 377:12110
58. Muthukrishnan N, Davim JP (2011) An investigation of the effect of work piece reinforcing percentage on the machinability of Al-SiC metal matrix composites. Free Radic Biol Med 49(1):15–24
59. Duan C, Sun W, Che M et al (2019) Effects of cooling and lubrication conditions on tool wear in turning of Al/SiC_p composite. Int J Adv Manuf Technol 103:1467–1479
60. Kalaichelvi V, Karthikeyan R, Sivakumar D et al (2012) Tool wear classification using fuzzy logic for machining of Al/SiC composite material. Model Numer Simul Mater Sci 2(2):28–36
61. Chavoshi SZ (2011) Tool flank wear prediction in CNC turning of 7075Al alloy SiC composite. Prod Eng Res Dev 5(1):37–47
62. Pramanik A, Zhang LC, Arsecularatne JA (2006) Prediction of cutting forces in machining of metal matrix composites. Int J Mach Tools Manuf 46(14):1795–1803
63. Antnio CAC, Davim JP (2002) Optimal cutting conditions in turning of particulate metal matrix composites based on experiment and a genetic search model. Compos A 33(2):213–219
64. Wang J, Zuo J, Shang Z et al (2019) Modeling of cutting force prediction in machining high-volume SiC_p/Al composites. Appl Math Model 70:1–17
65. Gaitonde VN, Karnik SR, Davim JP (2009) Some studies in metal matrix composites machining using response surface methodology. J Reinf Plast Compos 28(20):2445–2457
66. Krishnamurthy L, Sridhara BK, Abdulbudan D (2011) Comparative study on the machinability aspects of aluminium silicon carbide and aluminium graphite composites. Int J Mach Machinab Mater 10(7/8):137–152
67. Dabade UA, Dapkekar D, Joshi SS (2009) Modeling of chiptool interface friction to predict cutting forces in machining of Al/SiC_p composites. Int J Mach Tools Manuf 49(9):690–700
68. Ramasubramanian K, Arunachalam N, Rao MR (2019) Wear performance of nano-engineered boron doped graded layer CVD diamond coated cutting tool for machining of Al-SiC MMC. Wear 426:1536–1547
69. El-Gallab M, Sklad M (1998) Machining of Al/SiC particulate metal matrix composites: part II: workpiece surface integrity. J Mater Process Technol 83(13):277–285
70. Liu H, Wang S, Zong W (2019) Tool rake angle selection in micro-machining of 45 vol.% SiC_p/2024Al based on its brittle-plastic properties. J Manuf Process 37:556–562
71. Lin JT, Bhattacharyya D, Ferguson WG (1998) Chip formation in the machining of SiC-particle-reinforced aluminium-matrix composites. Compos Sci Technol 58(2):285–291
72. Hung NP, Yeo SH, Lee KK et al (1998) Chip formation in machining particle-reinforced metal matrix composites. Adv Manuf Process 13(1):85–100
73. Dabade UA, Joshi SS (2009) Analysis of chip formation mechanism in machining of Al/SiCp metal matrix composites. J Mater Process Technol 209(10):4704–4710
74. Ge YF, Xu JH, Fu YC (2010) Surface generation and chip formation when ultra-precision turning of SiC_p/Al composites. Adv Mater Res 135:282–287
75. Kishawy H, Kannan S, Balazinski M (2004) An energy based analytical force model for orthogonal cutting of metal matrix composites. CIRP Ann 53(1):91–94
76. Dandekar CR, Shin YC (2009) Multi-step 3-D finite element modeling of subsurface damage in machining particulate reinforced metal matrix composites. Compos A Appl Sci Manuf 40(8):1231–1239
77. Duan C, Sun W, Fu C et al (2018) Modeling and simulation of tool-chip interface friction in cutting Al/SiCp composites based on a three-phase friction model. Int J Mech Sci 142:384–396
78. Wu Q, Xu WX, Zhang LC (2019) Machining of particulate-reinforced metal matrix composites: an investigation into the chip formation and subsurface damage. J Mater Process Technol 274:116315
79. Wu Q, Xu W, Zhang L (2018) A micromechanics analysis of the material removal mechanisms in the cutting of ceramic particle reinforced metal matrix composites. Mach Sci Technol 22(4):638–651
80. Wang Y, Liao W, Yang K et al (2019) Simulation and experimental investigation on the cutting mechanism and surface generation in machining SiCp/Al MMCs. Int J Adv Manuf Technol 100(5/8):1393–1404
81. Guo H, Wang D, Zhou L (2011) FEM prediction of chip morphology during the machining of particulates reinforced Al matrix composites. Adv Mater Res 188:220–223
82. Fathipour M, Hamedi M, Yousefi R (2013) Numerical and experimental analysis of machining of Al (20 vol% SiC) composite by the use of abaqus software. Materialwiss Werkstofftech 44(1):14–20
83. Sandhiya YN, Thamizharasan M, Subramanyam BA et al (2018) Finite element analysis of tool particle interaction, particle volume fraction, size, shape and distribution in machining of A356/SiCp. Mater Today Proc 5(8):16800–16806
84. Dandekar CR, Shin YC (2012) Modeling of machining of composite materials: a review. Int J Mach Tools Manuf 57:102–121
85. Ge Y, Xu J, Yang H et al (2008) Workpiece surface quality when ultra-precision turning of SiC_p/Al composites. J Mater Process Technol 203(1/3):166–175
86. Davim JP (2002) Diamond tool performance in machining metal matrix composites. J Mater Process Technol 128(13):100–105
87. Pradhan S, Singh G, Bhagi LK (2018) Study on surface roughness in machining of Al/SiCp metal matrix composite using desirability function analysis approach. Mater Today Proc 5(14):28108–28116
88. Ding X, Liew WYH, Liu XD (2005) Evaluation of machining performance of MMC with PCBN and PCD tools. Wear 259(712):1225–1234
89. Sharma S (2013) Optimization of machining process parameters for surface roughness of Al-composites. J Inst Eng India Ser C 94(4):327–333

90. Davim JP (2003) Design of optimisation of cutting parameters for turning metal matrix composites based on the orthogonal arrays. J Mater Process Technol 132(1):340–344
91. Palanikumar K, Karthikeyan R (2007) Assessment of factors influencing surface roughness on the machining of Al/SiC particulate composites. Mater Des 28(5):1584–1591
92. Muthukrishnan N, Davim JP (2009) Optimization of machining parameters of Al/SiC-MMC with ANOVA and ANN analysis. J Mater Process Technol 209(1):225–232
93. Aurich JC, Zimmermann M, Schindler S et al (2016) Effect of the cutting condition and the reinforcement phase on the thermal load of the workpiece when dry turning aluminum metal matrix composites. Int J Adv Manuf Technol 82(5/8):1317–1334
94. Muthukrishnan N, Murugan M, Rao KP (2008) Machinability issues in turning of Al-SiC (10p) metal matrix composites. Int J Adv Manuf Technol 39(3/4):211–218
95. Ge YF, Xu JH, Yang H et al (2007) Machining induced defects and the influence factors when diamond turning of SiC_p/Al composites. Appl Mech Mater 10/12:626–630
96. Dabade U, Sonawane H, Joshi S (2010) Cutting force and surface roughness in machining Al/SiC composites of varying composition. Mach Sci Technol 14(2):258–279
97. Cheung CF, Chan KC, To S et al (2002) Effect of reinforcement in ultra-precision machining of Al6061/SiC metal matrix composites. Scr Mater 47(2):77–82
98. Wang Y, Liao W, Yang K et al (2019) Investigation on cutting mechanism of SiCp/Al composites in precision turning. Int J Adv Manuf Technol 100(1/4):963–972
99. Gnay M, Eker U (2011) Evaluation of surface integrity during machining with different tool grades of SiC_p/Al-Si composites produced by powder metallurgy. Mater Sci Forum 672:319–322
100. Muguthu JN, Gao D (2013) Profile fractal dimension and dimensional accuracy analysis in machining metal matrix composites (MMCs). Mater Manuf Process 28(10):1102–1109
101. Bushlya V, Filip Lenric, Gutnichenko O et al (2017) Performance and wear mechanisms of novel superhard diamond and boron nitride based tools in machining Al-SiCp metal matrix composite. Wear 376/377:152–164
102. Varadarajan YS, Vijayaraghavan L, Krishnamurthy R (2006) Performance enhancement through microwave irradiation of k20 carbide tool machining Al/SiC metal matrix composite. J Mater Process Technol 173(2):185–193
103. Shankar E, John MRS, Thirumurugan M et al (2008) Surface characteristics of Al(SiC)p metal matrix composites by roller burnishing process. Int J Mach Mach Mater 3(3/4):283–292
104. Sadat A (2009) On the quality of machined surface region when turning Al/SiC metal marix composites. Mach Sci Technol 13(3):338–355
105. Aurich JC, Zimmermann M, Schindler S et al (2016) Turning of aluminum metal matrix composites: influence of the reinforcement and the cutting condition on the surface layer of the workpiece. Adv Manuf 4(3):225–236
106. Bansal P, Upadhyay L (2016) Effect of turning parameters on tool wear, surface roughness and metal removal rate of alumina reinforced aluminum composite. Procedia Technology 23:304–310
107. Ramanujam R, Muthukrishnan N, Raju R (2011) Optimization of cutting parameters for turning Al-SiC(10p) MMC using ANOVA and gray relational analysis. Int J Precis Eng Manuf 12(4):651–656
108. Jeyapaul R, Sivasankar S (2011) Optimization and modeling of turning process for aluminium-silicon carbide composite using artificial neural network models. In: IEEE international conference on industrial engineering and engineering management, pp 773–778
109. Bhushan RK, Kumar S, Das S (2012) GA approach for optimization of surface roughness parameters in machining of Al alloy SiC particle composite. J Mater Eng Perform 21(8):1676–1686
110. Shetty R, Pai RB, Rao SS et al (2009) Taguchi's technique in machining of metal matrix composites. J Braz Soc Mech Sci Eng 31(1):12–20
111. Ramanujam R, Raju R, Muthukrishnan N (2010) Taguchi multimachining characteristics optimization in turning of Al-15% SiCp composites using desirability function analysis. J Stud Manuf 1(2/3):120–125
112. Manna A, Bhattacharyya B (2006) Taguchi method based optimization of cutting tool flank wear during turning of PR-Al/20vol% SiC-MMC. Int J Mach Machinab Mater 1(4):488–499
113. Sahoo AK, Pradhan S (2013) Modeling and optimization of Al/SiCp MMC machining using Taguchi approach. Measurement 46(9):3064–3072
114. Sahoo A, Pradhan S, Rout A (2013) Development and machinability assessment in turning Al/SiCp-metal matrix composite with multilayer coated carbide insert using Taguchi and statistical techniques. Arch Civ Mech Eng 13(1):27–35
115. Seeman M, Ganesan G, Karthikeyan R et al (2010) Study on tool wear and surface roughness in machining of particulate aluminum metal matrix composite-response surface methodology approach. Int J Adv Manuf Technol 48(5/8):613–624
116. Palanikumar K, Shanmugam K, Davim JP (2009) Analysis and optimization of cutting parameters for surface roughness in machining Al/SiC particulate composites by PCD tool. Int J Mater Prod Technol 37(1/2):117–128
117. Tamang S, Chandrasekaran M (2015) Modeling and optimization of parameters for minimizing surface roughness and tool wear in turning Al/SiCp MMC, using conventional and soft computing techniques. Adv Prod Eng Manag 10(2):59–72
118. Joardar H, Das N, Sutradhar G et al (2014) Application of response surface methodology for determining cutting force model in turning of LM6/SiCp metal matrix composite. Measurement 47:452–464
119. Chandrasekaran M, Tamang S (2014) Desirability analysis and genetic algorithm approaches to optimize single and multi response characteristics in machining Al-SiCp MMC. Aimtdr, p 653
120. Kumar S, Bhushan RK, Das S (2014) Machining performance of 7075 Al alloy SiC metal matrix composite with HSS and carbide tool. J Manuf Technol Res 5(1/2):17–41
121. Bhushan RK, Kumar S, Das S (2010) Effect of machining parameters on surface roughness and tool wear for 7075 Al alloy SiC composite. Int J Adv Manuf Technol 50(5/8):459–469
122. Kumar R, Chauhan S (2015) Study on surface roughness measurement for turning of Al 7075/10/SiCp and Al 7075 hybrid composites by using response surface methodology (RSM) and artificial neural networking (ANN). Measurement 65:166–180
123. Bhushan RK (2013) Optimization of cutting parameters for minimizing power consumption and maximizing tool life during machining of Al alloy SiC particle composites. J Clean Prod 39(1):242–254
124. Mohan B, Venugopal S, Rajadurai A et al (2008) Optimization of the machinability of the Al-SiC metal matrix composite using the dynamic material model. Metall Mater Trans A 39(12):2931–2940
125. Bian R, He N, Li L et al (2014) Precision milling of high volume fraction SiC_p/Al composites with monocrystalline diamond end mill. Int J Adv Manuf Technol 71(1/4):411–419
126. ClausB Nestler A, Schubert A (2016) Investigation of surface properties in milling of SiC particle reinforced aluminium matrix composites (AMCs). Procedia CIRP 46:480–483

127. Shen B, Sun FH, Zhang DC (2010) Comparative studies on the cutting performance of HFCVD diamond and DLC coated WC-Co milling tools in dry machining Al/SiC-MMC. Adv Mater Res 126:220–225
128. Huang S, Zhou L, Yu X et al (2012) Experimental study of high-speed milling of SiC_p/Al composites with PCD tools. Int J Adv Manuf Technol 62(5/8):487–493
129. Huang S, Guo L, He H et al (2018) Study on characteristics of SiC_p/Al composites during high-speed milling with different particle size of PCD tools. Int J Adv Manuf Technol 95(5/8):2269–2279
130. Wang YJ, Pan MQ, Chen T et al (2012) Performance of cutting tools in high speed milling of SiCp/Al composites. Adv Mater Res 591/593:311–314
131. Huang ST, Zhou L (2011) Evaluation of tool wear when milling SiC_p/Al composites. Eng Mater 455:226–231
132. Ge Y, Xu J, Fu Y (2015) Machinability of SiC particle reinforced 2009Al matrix composites when high-speed milling with PCD tools. Int J Mach Mach Mater 17(2):108–126
133. Deng B, Wang H, Peng F et al (2018) Experimental and theoretical investigations on tool wear and surface quality in micro milling of SiC_p/Al composites under dry and MQL conditions. In: ASME 2018 International Mechanical Engineering Congress and Exposition, american society of mechanical Engineers, pp V002T02A001–V002T02A001
134. Karthikeyan R, Raghukandan K, Naagarazan RS et al (2000) Optimizing the milling characteristics of Al-SiC particulate composites. Met Mater 6(6):539–547
135. Ekici E, Samta G, Glesin M (2014) Experimental and statistical investigation of the machinability of Al-10% SiC MMC produced by hot pressing method. Arab J Sci Eng 39(4):3289–3298
136. Jayakumar K, Mathew J, Joseph MA et al (2012) Processing and end milling behavioural study of A356-SiCp composite. Mater Sci Forum 710:338–343
137. Jayakumar K, Mathew J, Joseph MA (2013) An investigation of cutting force and tool-work interface temperature in milling of Al-SiCp metal matrix composite. Proc Inst Mech Eng Part B J Eng Manuf 227(3):362–374
138. Vallavi MA, Gandhi NMD, Velmurugan C (2018) Application of genetic algorithm in optimisation of cutting force of Al/SiCp metal matrix composite in end milling process. Int J Mater Prod Technol 56(3):234–252
139. Huang ST, Yu X, Zhou L (2011) Experimental study and modeling of milling force during high-speed milling of SiC_p/Al composites using regression analysis. Adv Mater Res 188:3–8
140. Babu BG, Selladurai V, Shanmugam R (2008) Analytical modeling of cutting forces of end milling operation on aluminum silicon carbide particulate metal matrix composite material using response surface methodology. J Eng Appl Sci 3(2):195–196
141. Chen X, Xie L, Xue X et al (2017) Research on 3D milling simulation of SiCp /Al composite based on a phenomenological model. Int J Adv Manuf Technol 92:2715–2723
142. Ge YF, Xu JH, Fu YC (2011) Cutting forces when high-speed milling of SiC_p/Al composites. Adv Mater Res 308:871–876
143. Huang S, Guo L, Yang H et al (2019) Study on characteristics in high-speed milling SiC_p/Al composites with small particles and high volume fraction by adopting PCD cutters with different grain sizes. Int J Adv Manuf Technol 95:1–9
144. Zha H, Feng P, Zhang J et al (2018) Material removal mechanism in rotary ultrasonic machining of high-volume fraction SiC_p/Al composites. Int J Adv Manuf Technol 97:1–11
145. Qin S, Cai XJ, Zhang YS et al (2012) Experimental studies on machinability of 14 wt.% of SiC particle reinforced aluminium alloy composites. Mater Sci Forum 723:94–98
146. Reddy NSK, Kwang-Sup S, Yang M (2008) Experimental study of surface integrity during end milling of Al/SiC particulate metal-matrix composites. J Mater Process Technol 201(1–3):574–579
147. Zhang GF, Tan YQ, Zhang B et al (2009) Effect of SiC particles on the machining of aluminum/SiC composite. Mater Sci Forum 626:219–224
148. Liu J, Cheng K, Ding H et al (2019) Realization of ductile regime machining in micro-milling SiC_p/Al composites and selection of cutting parameters. Proc Inst Mech Eng Part C J Mech Eng Sci 233(12):4336–4347
149. Chandrasekaran M (2012) Development of predictive model for surface roughness in end milling of Al-SiCp metal matrix composites using fuzzy logic. World Acad Sci Eng Technol 6(7):928–933
150. Reddy KS, Vijayaraghavan L (2011) Machining studies on milling of Al/SiCp composite. Int J Mach Mach Mater 9(1/2):116–130
151. Wang T, Xie L, Wang X (2015) 2D and 3D milled surface roughness of high volume fraction SiC_p/Al composites. Def Technol 11(2):104–109
152. Ghoreishi R, Roohi AH, Ghadikolaei AD (2018) Analysis of the influence of cutting parameters on surface roughness and cutting forces in high speed face milling of Al/SiC MMC. Mater Res Express 5(8):086521
153. Huang S, Guo L, He H et al (2018) Experimental study on SiC_p/Al composites with different volume fractions in high-speed milling with PCD tools. Int J Adv Manuf Technol 97(5/8):2731–2739
154. Wang T, Xie L, Wang X et al (2013) Surface integrity of high speed milling of Al/SiC/65p aluminum matrix composites. Procedia CIRP 8:475–480
155. Arokiadass R, Palaniradja K, Alagumoorthi N (2011) Prediction of flank wear in end milling of particulate metal matrix composite-RSM approach. Int J Appl Eng Res 6(5):559–569
156. Jeyakumar S, Marimuthu K, Ramachandran T (2013) Prediction of cutting force, tool wear and surface roughness of Al6061/SiC composite for end milling operations using RSM. J Mech Sci Technol 27(9):2813–2822
157. Krishna MV, Xavior MA (2015) Experiment and statistical analysis of end milling parameters for Al/SiC using response surface methodology. Int J Eng Technol 7:2274–2285
158. Rajeswari S, Sivasakthivel P (2018) Optimisation of milling parameters with multi-performance characteristic on Al/SiC metal matrix composite using grey-fuzzy logic algorithm. Multidiscip Model Mater Struct 14(2):284–305
159. Sujay P, Sankar BR, Umamaheswarrao P (2018) Experimental investigations on acceleration amplitude in end milling of Al6061-SiC metal matrix composite. Procedia Comput Sci 133:740–745
160. Ge YF, Xu JH, Fu YC (2011) Experimental study on high-speed milling of SiC_p/Al composites. Adv Mater Res 291/294:725–731
161. Wang T, Xie L, Wang X et al (2015) Pcd tool performance in high-speed milling of high volume fraction SiC_p/Al composites. Int J Adv Manuf Technol 78(9/12):1445–1453
162. Tosun G, Muratoglu M (2004) The drilling of an Al/SiCp metal-matrix composites. Part I: microstructure. Compos Sci Technol 64(2):299–308
163. Haq AN, Marimuthu P, Jeyapaul R (2008) Multi response optimization of machining parameters of drilling Al/SiC metal matrix composite using grey relational analysis in the Taguchi method. Int J Adv Manuf Technol 37(3/4):250–255
164. Monaghan J, O'reilly P (1992) The drilling of an Al/SiC metal-matrix composite. J Mater Process Technol 33(4):469–480

165. Barnes S, Pashby IR, Hashim AB (1999) Effect of heat treatment on the drilling performance of aluminium/SiC MMC. Appl Compos Mater 6(2):121–138
166. Thakre AA, Soni S (2016) Modeling of burr size in drilling of aluminum silicon carbide composites using response surface methodology. Eng Sci Technol Int J 19(3):1199–1205
167. Babu KV, Uthayakumar M, Jappes JTW et al (2015) Optimization of drilling process on Al-SiC composite using grey relation analysis. Int J Manuf Mater Mech Eng 5(4):17–31
168. Tosun G, Muratoglu M (2004) The drilling of Al/SiCp metal-matrix composites. Part 2: workpiece surface integrity. Compos Sci Technol 64(10/11):1413–1418
169. Calatoru V, Balazinski M, Mayer J et al (2008) Diffusion wear mechanism during high-speed machining of 7475-T7351 aluminum alloy with carbide end mills. Wear 265(11/12):1793–1800
170. Xiang J, Pang S, Xie L et al (2018) Mechanism based FE simulation of tool wear in diamond drilling of SiC_p/Al composites. Materials 11(2):252
171. Huang S, Zhou L, Chen L et al (2012) Drilling of SiC_p/Al metal matrix composites with polycrystalline diamond (PCD) tools. Mater Manuf Process 27(10):1090–1094
172. Hu F, Xie L, Xiang J et al (2018) Finite element modelling study on small-hole peck drilling of SiC_p/Al composites. Int J Adv Manuf Technol 96(9/12):3719–3728
173. Zhou L, Huang S, Xu L et al (2013) Drilling characteristics of SiC_p/Al composites with electroplated diamond drills. Int J Adv Manuf Technol 69(5/8):1165–1173
174. Tosun G (2011) Statistical analysis of process parameters in drilling of Al/SiC metal matrix composite. Int J Adv Manuf Technol 55(5/8):477–485
175. Barnes S, Pashby IR (2000) Through-tool coolant drilling of aluminum/SiC metal matrix composite. J Eng Mater Technol 122(4):384–388
176. Somasundaram G, Boopathy SR (2010) Fabrication and friction drilling of aluminum silicon carbide metal matrix composite. In: Frontiers in automobile and mechanical engineering-2010. IEEE, pp 21–26
177. Somasundaram G, Boopathy RS, Palanikumar K (2012) Modeling and analysis of roundness error in friction drilling of aluminum silicon carbide metal matrix composite. J Compos Mater 46(2):169–181
178. Singh S, Singh I, Dvivedi A (2013) Multi objective optimization in drilling of Al6063/10% SiC metal matrix composite based on grey relational analysis. Proc Inst Mech Eng Part B J Eng Manuf 227(12):1767–1776
179. Karthikeyan R, Jaiganesh S, Pai B (2002) Optimization of drilling characteristics for Al/SiCp composites using fuzzy/GA. Met Mater Int 8(2):163–168
180. Dhavamani C, Alwarsamy T (2012) Optimization of machining parameters for aluminum and silicon carbide composite using genetic algorithm. Procedia Eng 38:1994–2004
181. Singh H, Kamboj A, Kumar S (2014) Multi response optimization in drilling Al6063/SiC/15% metal matrix composite. Int J Chem Nucl Mater Metall Eng 8(4):281–286
182. Ekici E, Motorcu AR (2014) Evaluation of drilling Al/SiC composites with cryogenically treated HSS drills. Int J Adv Manuf Technol 74(9/12):1495–1505
183. Davim JP, Antonio CC (2001) Optimisation of cutting conditions in machining of aluminium matrix composites using a numerical and experimental model. J Mater Process Technol 112(1):78–82
184. Zhou L, Huang ST, Yu XL (2011) Experimental study of grinding characteristics on SiC_p/Al composites. Key Eng Mater 487:135–139
185. Huang S, Yu X, Wang F et al (2015) A study on chip shape and chipforming mechanism in grinding of high volume fraction SiC particle reinforced Al-matrix composites. Int J Adv Manuf Technol 80(9/12):1927–1932
186. Ilio AD, Paoletti A (2000) A comparison between conventional abrasives and superabrasives in grinding of SiC-aluminium composites. Int J Mach Tools Manuf 40(2):173–184
187. Zhang GF, Zhang B, Deng ZH (2009) Mechanisms of Al/SiC composite machining with diamond whiskers. Key Eng Mater 404:165–175
188. Xu LF, Zhou L, Yu XL et al (2011) An experimental study on grinding of SiC/Al composites. Adv Mater Res 188:90–93
189. Zhong ZW (2003) Grinding of aluminium-based metal matrix composites reinforced with Al_2O_3 or SiC particles. Int J Adv Manuf Technol 21(2):79–83
190. Ilio AD, Paoletti A, Tagliaferri V et al (1996) An experimental study on grinding of silicon carbide reinforced aluminium alloys. Int J Mach Tools Manuf 36(6):673–685
191. Zhou L, Huang S, Yu X (2014) Machining characteristics in cryogenic grinding of SiC_p/Al composites. Acta Metall Sin 27(5):869–874
192. Kumar KR, Vettivel S (2014) Effect of parameters on grinding forces and energy while grinding Al (A356)/SiC composites. Tribol-Mater Surf Interfaces 8(4):235–240
193. Lu S, Gao H, Bao Y et al (2019) A model for force prediction in grinding holes of SiC_p/Al composites. Int J Mech Sci 160:1–14
194. Thiagarajan C, Somasundaram S, Shankar P (2013) Effect of grinding temperature during cylindrical grinding on surface finish of Al/SiC metal matrix composites. Int J Eng Sci 2(12):58–66
195. Sun FH, Li X, Wang Y et al (2006) Studies on the grinding characteristics of SiC particle reinforced aluminum-based mmcs. Key Eng Mater 304:261–265
196. Zhou L, Huang S, Zhang C (2013) Numerical and experimental studies on the temperature field in precision grinding of SiC_p/Al composites. Int J Adv Manuf Technol 67(5/8):1007–1014
197. Du J, Zhang H, He W et al (2019) Simulation and experimental study on surface formation mechanism in machining of SiC_p/Al composites. Appl Compos Mater 26(1):29–40
198. Yin G, Wang D, Cheng J (2019) Experimental investigation on micro-grinding of SiC_p/Al metal matrix composites. Int J Adv Manuf Technol 102:1–15
199. Chandrasekaran H, Johansson JO (1997) Influence of processing conditions and reinforcement on the surface quality of finish machined aluminium alloy matrix composites. CIRP Ann 46(1):493–496
200. Zhu CM, Gu P, Wu YY et al (2019) Surface roughness prediction model of SiC_p/Al composite in grinding. Int J Mech Sci 155:98–109
201. Pai D, Rao SS, Shetty R (2011) Application of statistical tool for optimization of specific cutting energy and surface roughness on surface grinding of AlSiC35p composites. Int J Sci Stat Comput 2(1):16–32
202. Hung N, Zhong Z, Zhong C (1997) Grinding of metal matrix composites reinforced with silicon-carbide particles. Mater Manuf Process 12(6):1075–1091
203. Nandakumar A, Rajmohan T, Vijayabhaskar S (2019) Experimental evaluation of the lubrication performance in MQL grinding of nano SiC reinforced al matrix composites. Silicon 11:1–13
204. Li JG, Du JG, Yao YX (2012) A comparison of dry and wet machining of SiC particle-reinforced aluminum metal matrix composites. Adv Mater Res 500:168–173
205. Du J, Zhou L, Li J et al (2014) Analysis of chip formation mechanism in mill-grinding of SiC_p/Al composites. Mater Manuf Processe 29(11/12):1353–1360

206. Du J, Li J, Yao Y et al (2014) Prediction of cutting forces in mill-grinding SiC_p/Al composites. Mater Manuf Process 29(3):314–320
207. Yao Y, Du JG, Li JG et al (2011) Surface quality analysis in millgrinding of SiC_p/Al. Adv Mater Res 299:1060–1063
208. Li J, Du J, Yao Y et al (2014) Experimental study of machinability in mill-grinding of SiC_p/Al composites. J Wuhan Univ Technol-Mater Sci Ed 29(6):1104–1110
209. Li JG, Du JG, Zhao H (2011) Experimental study on the surface roughness with mill-grinding SiC particle reinforced aluminum matrix composites. Adv Mater Res 188:203–207
210. Thiagarajan C, Sivaramakrishnan R, Somasundaram S (2012) Modeling and optimization of cylindrical grinding of Al/SiC composites using genetic algorithms. J Braz Soc Mech Sci Eng 34(1):32–40
211. Yao YX, Du JG, Li JG (2012) Investigation of material removal rate in mill-grinding SiC particle reinforced aluminum matrix composites. Adv Mater Res 500:320–325
212. Thiagarajan C, Sivaramakrishnan R, Somasundaram S (2011) Experimental evaluation of grinding forces and surface finish in cylindrical grinding of Al/SiC metal matrix composites. Proc Inst Mech Eng Part B J Eng Manuf 225(9):1606–1614
213. Huang S, Zhou L, Yu X et al (2012) Study of the mechanism of ductileregime grinding of SiC_p/Al composites using finite element simulation. Int J Mater Res 103(10):1210–1217
214. Kathiresan M, Sornakumar T (2010) EDM studies on aluminum alloy-silicon carbide composites developed by vortex technique and pressure die casting. J Miner Mater Charact Eng 9(1):79
215. Ming W, Ma J, Zhang Z et al (2016) Soft computing models and intelligent optimization system in electro-discharge machining of SiC/Al composites. Int J Adv Manuf Technol 87(1/4):1–17
216. Karthikeyan R, Raju S, Naagarazan RS et al (2001) Optimization of electrical discharge machining characteristics of SiCp/LM25Al composites using goal programming. J Mater Sci Technol 17(s1):S57–S60
217. Dev A, PatelK Pandey PM et al (2009) Machining characteristics and optimisation of process parameters in micro-EDM of SiCp/ Al composites. Int J Manuf Res 4(4):458–480
218. Singh B, Kumar J, Kumar S (2013) Investigating the influence of process parameters of ZNC EDM on machinability of A6061/10% SiC composite. Adv Mater Sci Eng. https://doi.org/10.1155/2013/173427
219. Seo YW, Kim D, Ramulu M (2006) Electrical discharge machining of functionally graded 15–35 vol% SiC_p/Al composites. Adv Manuf Process 21(5):479–487
220. Dhar S, Purohit R, Saini N et al (2007) Mathematical modeling of electric discharge machining of cast Al-4Cu-6Si alloy-10 wt.% SiCp composites. J Mater Process Technol 194(1/3):24–29
221. Ramulu M, Paul G, Patel J (2001) EDM surface effects on the fatigue strength of A 15 vol% SiC/Al metal matrix composite material. Compos Struct 54(1):79–86
222. Uthayakumar M, Babu KV, Kumaran ST et al (2019) Study on the machining of Al-SiC functionally graded metal matrix composite using die-sinking EDM. Part Sci Technol 37(1):103–109
223. Dvivedi A, Kumar P, Singh I (2010) Effect of EDM process parameters on surface quality of Al 6063 SiCp metal matrix composite. Int J Mater Prod Technol 39(3/4):357–377
224. Yu P, Xu J, Li Y et al (2018) Electrical discharge machining of SiCp/2024Al composites. In: 2018 IEEE international conference on manipulation. manufacturing and measurement on the nanoscale (3MNANO). pp 192–196
225. Khan F, Singh B, Kalra C (2012) Experimental investigation of machining of Al/SiC MMC on EDM by using rotating and non-rotating electrode. Int J IT 1:50–53
226. Singh NK, Prasad R, Johari D (2018) Electrical discharge drilling of Al-SiC composite using air assisted rotary tubular electrode. Mater Today Proc 5(11):23769–23778
227. Sidhu SS, Batish A, Kumar S (2013) Neural network-based modeling to predict residual stresses during electric discharge machining of Al/SiC metal matrix composites. Proc Inst Mech Eng Part B J Eng Manuf 227(11):1679–1692
228. Fard RK, Afza RA, Teimouri R (2013) Experimental investigation, intelligent modeling and multi-characteristics optimization of dry WEDM process of AlSiC metal matrix composite. J Manuf Process 15(4):483–494
229. Bhuyan RK, Routara BC, Parida AK (2015) Using entropy weight, OEC and fuzzy logic for optimizing the parameters during EDM of Al-24 % SiCp MMC. Adv Prod Eng Manag 10(4):217–227
230. Golshan A, Gohari S, Ayob A (2012) Multi-objective optimisation of electrical discharge machining of metal matrix composite Al/SiC using nondominated sorting genetic algorithm. Int J Mechatron Manuf Syst 5(5/6):385–398
231. SatpathyA Tripathy S, Senapati NP et al (2017) Optimization of EDM process parameters for AlSiC-20% SiC reinforced metal matrix composite with multi response using topsis. Mater Today Proc 4(2):3043–3052
232. Puhan D, Mahapatra SS, Sahu J et al (2013) A hybrid approach for ultiresponse optimization of non-conventional machining on AlSiCp MMC. Measurement 46(9):3581–3592
233. Bhuyan RK, Routara BC, Parida AK (2015) An approach for optimization the process parameter by using topsis method of Al24%SiC metal matrix composite during EDM. Mater Today Proc 2(4/5):3116–3124
234. Bhuyan RK, RoutaraB, Parida AK et al (2014) Parametric optimization of Al-SiC12% metal matrix composite machining by electrical discharge machine. In: India manufacturing technology design and research conference, pp 345–345
235. Raza MH, Wasim A, Ali MA et al (2018) Investigating the effects of different electrodes on Al6061-SiC-7.5 wt% during electric discharge machining. Int J Adv Manuf Technol 99(9/12):3017–3034
236. Gopalakannan S, Senthilvelan T (2013) EDM of cast Al/SiC metal matrix nanocomposites by applying response surface method. Int J Adv Manuf Technol 67(1/4):485–493
237. Balasubramaniam V, Baskar N, Narayanan CS (2016) Experimental investigations on EDM process for optimum cylindricity and SR through less machining time for Al6061/SiC composites. Asian J Res Soc Sci Humanit 6(12):126–134
238. Singh PN, Raghukandan K, Pai BC (2004) Optimization by grey relational analysis of EDM parameters on machining Al10%SiC composites. J Mater Process Technol 155/156(6):1658–1661
239. Murugesan S, Balamurugan K (2012) Optimization by grey relational analysis of EDM parameters in machining Al-15% SiC MMC using multihole electrode. J Appl Sci 12(10):963–970
240. Senapati NP, Kumar R, Tripathy S et al (2017) Multi-objective optimization of EDM process parameters using PCA and topsis method during the machining of Al-20% SiCp metal matrix composite. In: Innovative design and development practices in aerospace and automotive engineering, pp 359–367
241. Mohan B, Rajadurai A, Satyanarayana KG (2002) Effect of SiC and rotation of electrode on electric discharge machining of AlSiC composite. J Mater Process Technol 124(3):297–304
242. Vishwakarma U, Dvivedi A, Kumar P (2013) Finite element modeling of material removal rate in powder mixed electric discharge machining of Al-SiC metal matrix composites. Materials processing fundamentals. Springer, Cham, pp 151–158

243. Zhao WS, Meng QG, Wang ZL (2002) Application research on powder mixed EDM in rough machining. J Mater Process Technol 129(s1):30–33
244. Kansal H, Singh S, Kumar P (2007) Effect of silicon powder mixed EDM on machining rate of AISI D2 die steel. J Manuf Process 9(1):13–22
245. Kansal HK (2006) An experimental study of the machining parameters in powder mixed electric discharge machining of Al10%SiC metal matrix composites. Int J Mach Mach Mater 1(4):396–411
246. Hu QF, Song YB, Hou JP et al (2013) Surface properties of SiC_p/Al composite by powder-mixed EDM. Procedia CIRP 6:101–106
247. Singh B, Kumar J, Kumar S (2015) Influences of process parameters on MRR improvement in simple and powder-mixed EDM of AA6061/10% SiC composite. Mater Manuf Process 30(3):303–312
248. Singh B, Kumar J, Kumar S (2016) Investigation of the tool wear rate in tungsten powder-mixed electric discharge machining of AA6061/10% SiCp composite. Mater Manuf Process 31(4):456–466
249. Singh B, Kumar J, Kumar S (2014) Experimental investigation on surface characteristics in powder-mixed electrodischarge machining of AA6061/10% SiC composite. Mater Manuf Process 29(3):287–297
250. Mohal S, Kumar H (2017) Study on the multiwalled carbon nano tube mixed EDM of Al-SiCp metal matrix composite. Mater Today Procedings 4(2):3987–3993
251. Mohal S, Kumar H (2017) Parametric optimization of multiwalled carbon nanotube-assisted electric discharge machining of Al-10% SiCp metal matrix composite by response surface methodology. Mater Manuf Process 32(3):263–273
252. Vishwakarma UK, Dvivedi A, Kumar P (2014) Comparative study of powder mixed EDM and rotary tool EDM performance during machining of Al-SiC metal matrix composites. Int J Mach Mach Mater 16(2):113–128
253. Arya RK, Dvivedi A, Karunakar DB (2012) Parametric investigation of powder mixed electrical discharge machining of Al-SiC metal matrix composites. Int J Eng Innov Res 1(6):559–566
254. Mohanty S, Routara B, Nanda B et al (2018) Study of machining characteristics of Al-SiCp12% composite in nano powder mixed dielectric electrical discharge machining using RSM. Mater Today Proc 5(11):25581–25590
255. Behera S, Satapathy S, Ghadai SK (2015) Parameter optimisation of powder mixed EDM of aluminium-based metal matrix composite using Taguchi and grey analysis. Int J Prod Qual Manag 16(2):148–168
256. Mohanty S, Routara BC, Bhuayan RK (2017) Experimental investigation of machining characteristics for Al-SiC12% composite in electro-discharge machining. Mater Today Proc 4(8):8778–8787
257. Kumar H, Davim JP (2011) Role of powder in the machining of Al-10 matrix composites by powder mixed electric discharge machining. J Compos Mater 45(2):133–151
258. Pramanik A, Basak AK (2016) Degradation of wire electrode during electrical discharge machining of metal matrix composites. Wear 346/347:124–131
259. Adithan M (2009) Unconventional machining processes. Atlantic Publishers & Distributors, Chennai
260. Satishkumar D, Kanthababu M, Vajjiravelu V et al (2011) Investigation of wire electrical discharge machining characteristics of Al6063/SiC composites. Int J Adv Manuf Technol 56(9/12):975–986
261. Rozenek M, Kozak J, Dabrowski L et al (2001) Electrical discharge machining characteristics of metal matrix composites. J Mater Process Technol 109(3):367–370
262. Shandilya P, Jain PK, Jain NK (2012) On wire breakage and microstructure in WEDC of SiCp /6061 aluminum metal matrix composites. Int J Adv Manuf Technol 61(9/12):1199–1207
263. Patil NG, Brahmankar P (2010) Determination of material removal rate in wire electro-discharge machining of metal matrix composites using dimensional analysis. Int J Adv Manuf Technol 51(5/8):599–610
264. Ebeid S, Fahmy R, Habib S (2004) Mathematical modelling for wire electrical discharge machining of aluminum-silicon carbide composites. In: Proceedings of the 34th international MATADOR conference. Springer, pp 147–152
265. Yang WS, Chen GQ, Wu P et al (2017) Electrical discharge machining of Al2024-65 vol% SiC composites. Acta Metall Sin (Eng Lett) 30(5):1–9
266. Pramanik A (2016) Electrical discharge machining of MMCs reinforced with very small particles. Mater Manuf Process 31(4):397–404
267. Patil N, Brahmankar P (2006) Some investigations into wire electro-discharge machining performance of Al/SiCp composites. Int J Mach Mach Mater 1(4):412–431
268. Wang ZL, Geng XS, Chi GX et al (2014) Surface integrity associated with SiC/Al particulate composite by micro-wire electrical discharge machining. Mater Manuf Process 29(5):532–539
269. Kanthababu M, Jegaraj JJR, Gowri S (2016) Investigation on material removal rate and surface roughness in electrical discharge turning process of Al 7075-based metal matrix composites. Int J Manuf Technol Manag 30(3/4):216–239
270. Shandilya P, Jain P, Jain N (2012) Neural network based modeling in wire electric discharge machining of SiCp/6061 aluminum metal matrix composite. Adv Mater Res 383:6679–6683
271. Shandilya P, Jain PK, Jain NK (2012) Study on wire electric discharge machining based on response surface methodology and genetic algorithm. Adv Mater Res 622/623:1280–1284
272. Shandilya P, Jain PK, Jain NK (2013) RSM and ANN modeling approaches for predicting average cutting speed during WEDM of SiCp /6061 Al MMC. Procedia Eng 64:767–774
273. Patil N, Brahmankar P (2010) On the response surface modeling of wire electrical discharge machining of Al/SiCp metal matrix composites (MMCs). J Mach Form Technol 2(1/2):47–70
274. Srivastava A, Dixit AR, Tiwari S (2014) Experimental investigation of wire EDM process parameteres on aluminum metal matrix composite Al2024/SiC. Int J Adv Res Innov 2:511–515
275. Saini V, Khan ZA, Siddiquee AN (2013) Optimization of wire electric discharge machining of composite material (Al6061/SiCp) using Taguchi method. Int J Mech Prod Eng 2(1):61–64
276. Phate MR, Toney SB, Phate VR (2019) Analysis of machining parameters in wedm of Al/SiCp20 MMC using Taguchi-based grey-fuzzy approach. Modell Simul Eng 2019:1–13
277. Geng XS, Wang YK, Song BY et al (2013) Optimization and analysis for surface roughness of SiC_p/Al metal matrix composite by microWEDM. Adv Mater Res 821:1266–1270
278. Babu KA, Venkataramaiah P (2015) Multi-response optimization in wire electrical discharge machining (WEDM) of Al6061/SiCp composite using hybrid approach. J Manuf Sci Prod 15(4):327–338
279. Rao TB, Krishna AG (2014) Selection of optimal process parameters in WEDM while machining Al7075/SiCp metal matrix composites. Int J Adv Manuf Technol 73(1/4):299–314
280. Chen J, Gu L, Xu H et al (2015) Research on the machining performance of SiC/Al composites utilizing the beam process. In: ASME 2015 international manufacturing science and engineering conference, p V001T02A046

281. Chen J, Gu L, Liu X et al (2018) Combined machining of SiC/Al composites based on blasting erosion arc machining and CNC milling. Int J Adv Manuf Technol 96(1/4):111–121
282. Gu L, Chen J, Xu H et al (2016) Blasting erosion arc machining of 20 vol% SiC/Al metal matrix composites. Int J Adv Manuf Technol 87(9/12):2775–2784
283. Chen J, Gu L, Zhu Y et al (2017) High efficiency blasting erosion arc machining of 50 vol% SiC/Al matrix composites. Proc Inst Mech Eng Part B J Eng Manuf. https://doi.org/10.1177/0954405417690553
284. Chen J, Gu L, Xu H et al (2016) Study on blasting erosion arc machining of Ti6Al4V alloy. Int J Adv Manuf Technol 85(9/12):2819–2829
285. Xu H, Gu L, Chen J et al (2015) Machining characteristics of nickel-based alloy with positive polarity blasting erosion arc machining. Int J Adv Manuf Technol 79(5/8):937–947
286. Kozak J (1998) Mathematical models for computer simulation of electrochemical machining processes. J Mater Process Technol 76(1/3):170–175
287. Hackert-Oschätzchen M, Lehnert N, Maritn A et al (2016) Surface characterization of particle reinforced aluminum-matrix composites finished by pulsed electrochemical machining. Procedia CIRP 45:351–354
288. Kumar KS, Sivasubramanian R (2011) Modeling of metal removal rate in machining of aluminum matrix composite using artificial neural network. J Compos Mater 45(22):2309–2316
289. Senthilkumar C, Ganesan G, Karthikeyan R (2009) Study of electrochemical machining characteristics of Al/SiCp composites. Int J Adv Manuf Technol 43(3/4):256–263
290. Senthilkumar C, Ganesan G, Karthikeyan R et al (2010) Modelling and analysis of electrochemical machining of cast Al/20% SiCp composites. Mater Sci Technol 26(3):289–296
291. Dharmalingam S, Marimuthu P, Raja K et al (2014) Experimental investigation on electrochemical micro machining of Al-10wt% SiCp based on Taguchi design of experiments. J Rev Mech Eng 8(1):80–88
292. Lehnert N, Meichsner G, Hackert-Oschätzchen M et al (2018) Study on the influence of the processing speed in the generation of complex geometries in aluminium matrix composites by electrochemical precision machining. Procedia CIRP 68:713–718
293. Miller F, Monaghan J (2000) Non-conventional machining of particle reinforced metal matrix composite. Int J Mach Tools Manuf 40(9):1351–1366
294. Parikh PJ, Lam SS (2009) Parameter estimation for abrasive water jet machining process using neural networks. Int J Adv Manuf Technol 40(5/6):497–502
295. Kanca MKE, Eyercioglu O (2011) Prediction of surface roughness in abrasive waterjet machining of particle reinforced MMCs using genetic expression programming. Int J Adv Manuf Technol 55(9/12):955–968
296. Axinte D, Srinivasu D, Kong M et al (2009) Abrasive water jet cutting of polycrystalline diamond: a preliminary investigation. Int J Mach Tools Manuf 49(10):797–803
297. Hamatani G, Ramulu M (1990) Machinability of high temperature composites by abrasive waterjet. J Eng Mater Technol 112(4):381–386
298. Srinivas S, Babu NR (2011) Role of garnet and silicon carbide abrasives in abrasive waterjet cutting of aluminum-silicon carbide particulate metal matrix composites. Int J Appl Res Mech Eng 1:109–122
299. Srinivas S, Babu NR (2012) Penetration ability of abrasive waterjets in cutting of aluminum-silicon carbide particulate metal matrix composites. Mach Sci Technol 16(3):337–354
300. Patel R, Srinivas S (2017) Abrasive water jet turning of aluminum-silicon carbide metal matrix composites. In: Proceedings of 10th international conference on precision, meso, micro and nano engineering
301. Sharma V, Kumar V (2016) Multi-objective optimization of laser curve cutting of aluminium metal matrix composites using desirability function approach. J Braz Soc Mech Sci Eng 38(4):1221–1238
302. Sharma V, Kumar V (2018) Investigating the quality characteristics of Al5052/SiC metal matrix composites machined by Co_2 laser curve cutting. Proc Inst Mech Eng Part L J Mater Des Appl 232(1):3–19
303. Biffi C, Capello E, Previtali B (2009) Laser and lathe thread cutting of aluminium metal matrix composite. Int J Mach Mach Mater 6(3/4):250–269
304. Padhee S, Pani S, Mahapatra S (2012) A parametric study on laser drilling of Al/SiCp metal-matrix composite. Proc Inst Mech Eng Part B J Eng Manuf 226(1):76–91
305. Hackert-Oschätzchen M, Meichsner G, Zinecker M et al (2012) Micro machining with continuous electrolytic free jet. Precis Eng 36(4):612–619
306. Hackert-Oschätzchen M, Paul R, Kowalick M et al (2015) Multiphysics simulation of the material removal in jet electrochemical machining. Procedia CIRP 31:197–202
307. Hackert-Oschätzchen M, Paul R, Martin A (2015) Study on the dynamic generation of the jet shape in jet electrochemical machining. J Mater Process Technol 223:240–251
308. Lehnert N, Hackert-Oschätzchen M, Martin A et al (2018) Derivation of guidelines for reliable finishing of aluminium matrix composites by jet electrochemical machining. Procedia CIRP 68:471–476
309. Hackert-Oschätzchen M, Lehnert N, Martin A et al (2016) Jet electrochemical machining of particle reinforced aluminum matrix composites with different neutral electrolytes. IOP Conf Ser Mater Sci Eng 118:012036
310. Przestacki D, Szymański P (2011) Metallographic analysis of surface layer after turning with laser-assisted machining of composite A359/20SiCp. Composites 2:102–106
311. Dandekar CR, Shin YC (2013) Multi-scale modeling to predict sub-surface damage applied to laser-assisted machining of a particulate reinforced metal matrix composite. J Mater Process Technol 213(2):153–160
312. Zhang H, Kong X, Yang L et al (2015) High temperature deformation mechanisms and constitutive modeling for Al/SiCp/45 metal matrix composites undergoing laser-assisted machining. Mater Sci Eng A 642:330–339
313. Wang Z, Xu J, Yu H et al (2018) Process characteristics of laserassisted micro machining of SiCp/2024Al composites. Int J Adv Manuf Technol 94(9/12):3679–3690
314. Mirshamsi S, Movahhedy M, Khodaygan S (2019) Experimental modeling and optimizing process parameters in the laser assisted machining of silicon carbide particle-reinforced aluminum matrix composites. Mater Res Express 6(8):086591
315. Przestacki D (2014) Conventional and laser assisted machining of composite A359/20SiCp. Procedia Cirp 14:229–233
316. Kong X, Yang L, Zhang H et al (2017) Optimization of surface roughness in laser-assisted machining of metal matrix composites using Taguchi method. Int J Adv Manuf Technol 89(1/4):529–542
317. Kawalec M, Przestacki D, Bartkowiak K et al (2008) Laser assisted machining of aluminium composite reinforced by SiC particle. Int Congr Appl Lasers Electro-Opt. https://doi.org/10.2351/1.5061278
318. Kong X, Zhang H, Yang L et al (2016) Carbide tool wear mechanisms in laser-assisted machining of metal matrix composites. Int J Adv Manuf Technol 85(1/4):365–379

319. Bo Z, Liu CS, Zhu XS et al (2002) Research on vibration cutting performance of particle reinforced metallic matrix composites SiC/Al. J Mater Process Technol 129(s1):380–384
320. Zhong Z, Lin G (2006) Ultrasonic assisted turning of an aluminium-based metal matrix composite reinforced with SiC particles. Int J Adv Manuf Technol 27(11/12):1077–1081
321. Kim J, Bai W, Roy A et al (2019) Hybrid machining of metal-matrix composite. Procedia CIRP 82:184–189
322. Xiang DH, Zhi XT, Yue GX et al (2010) Study on surface quality of Al/SiCp composites with ultrasonic vibration high speed milling. Appl Mech Mater 42:363–366
323. Zhi XT, Xiang DH, Deng JQ (2013) Research on high volume fraction SiC_p/Al removal mechanism under condition of ultrasonic vertical vibration. Appl Mech Mater 373/375:2038–2041
324. Xu XX, Mo YL, Liu CS et al (2009) Drilling force of SiC particle reinforced aluminum-matrix composites with ultrasonic vibration. Key Eng Mater 416:243–247
325. Kadivar MA, Yousefi R, Akbari J et al (2012) Burr size reduction in drilling of Al/SiC metal matrix composite by ultrasonic assistance. Adv Mater Res 410:279–282
326. Xiang DH, Zhang YL, Yang GB et al (2014) Study on grinding force of high volume fraction SiC_p/Al composites with rotary ultrasonic vibration grinding. Adv Mater Res 1027:48–51
327. Zhou M, Zheng W (2016) A model for grinding forces prediction in ultrasonic vibration assisted grinding of SiC_p/Al composites. Int J Adv Manuf Technol 87(9/12):3211–3224
328. Zheng W, Zhou M, Zhou L (2017) Influence of process parameters on surface topography in ultrasonic vibration-assisted end grinding of SiC_p/Al composites. Int J Adv Manuf Technol 91(5/8):2347–2358
329. Zhou M, Wang M, Dong G (2016) Experimental investigation on rotary ultrasonic face grinding of SiC_p/Al composites. Adv Manuf Process 31(5):673–678
330. Shanawaz AM, Sundaram S, Pillai UTS et al (2011) Grinding of aluminium silicon carbide metal matrix composite materials by electrolytic in-process dressing grinding. Int J Adv Manuf Technol 57(1/4):143–150
331. Yu X, Huang S, Xu L (2016) Elid grinding characteristics of SiC_p/Al composites. Int J Adv Manuf Technol 86(5/8):1165–1171
332. Agrawal SS, Yadava Vinod (2013) Modeling and prediction of material removal rate and surface roughness in surface-electrical discharge diamond grinding process of metal matrix composites. Adv Manuf Process 28(4):381–389
333. Agrawal SS, Yadava V (2015) Development and experimental study of surface electrical discharge diamond grinding of Al10 wt%SiC composite. J Inst Eng 97(1):1–9
334. Marimuthu S, Dunleavey J, Liu Y et al (2019) Waterjet guided laser drilling of SiC reinforced aluminium metal matrix composites. J Compos Mater 53(26/27):3787–3796
335. Liu J, Yue T, Guo Z (2010) An analysis of the discharge mechanism in electrochemical discharge machining of particulate reinforced metal matrix composites. Int J Mach Tools Manuf 50(1):86–96

Ji-Peng Chen received his Ph.D. degree from the State Key Laboratory of Mechanical System and Vibration, School of Mechanical Engineering, Shanghai Jiao Tong University, China. He is currently an assistant professor at School of Mechanical and Electronic Engineering, Nanjing Forestry University, China, and a visiting scholar at Politecnico di Milano, Italy. His research interests include advanced manufacturing technology.

Lin Gu received his Ph.D. degree in Engineering from Harbin Institute of Technology. He iscurrently an associate professor in the State Key Laboratory of Mechanical System and Vibration,School of Mechanical Engineering, Shanghai Jiao Tong University, China. His research interestsinclude advanced manufacturing technology.

Guo-Jian He is a Ph.D. candidate at the State Key Laboratory of Mechanical System and Vibration,School of Mechanical Engineering, Shanghai Jiao Tong University, China. His research interestsinclude the technical and equipment of micro-EDM and arc discharge machining (ADM).